Fraunhofer
ISE

FRAUNHOFER INSTITUTE FOR SOLAR ENERGY SYSTEMS ISE

STUDY ON THE POSSIBLE YIELD GAIN BY INVERTERS WITH MULTI-MPPT COMPARED TO SINGLE-MPPT INVERTERS FOR DIFFERENT SOLAR SYSTEM CONFIGURATIONS AND LOCATIONS

Vergleich von Wechselrichtern mit Multi-MPPT und Single-MPPT für verschiedene Solaranlagenkonfigurationen und Standorte

STUDY ON THE POSSIBLE YIELD GAIN WITH INVERTERS WITH MULTI-MPPT COMPARED TO SINGLE-MPPT INVERTERS FOR DIFFERENT SOLAR SYSTEM CONFIGURATIONS AND LOCATIONS

Vergleich von Wechselrichtern mit Multi-MPPT und Single-MPPT für verschiedene Solaranlagenkonfigurationen und Standorte

Dipl.-Ing. Andreas Hensel
Dipl.-Ing. Leonhard Probst
Prof. Dr. Bruno Burger

Fraunhofer Institute for Solar Energy Systems ISE
in Freiburg.

Projektnummer: -
Auftraggeber: KACO new energy GmbH

About KACO new energy:

KACO new energy, a subsidiary of Siemens AG, is headquartered in Neckarsulm, Germany, and one of the world's largest manufacturers of inverters for grid-feed solar power. The product line-up recommends itself for the full power spectrum from PV systems for single-family homes and commercial and industrial enterprises to solar parks producing megawatts of electricity. Since 1999, KACO new energy has supplied inverters with a cumulative power output of more than 16 gigawatts. KACO new energy is the first company in the photovoltaic industry to achieve CO2-neutral production. In 2014, KACO new energy celebrated the 100th birthday of the original parent company which, at the end of the 1930s, was one of first ever inverter manufacturers. Recently, KACO new energy has received the seal as Top Brand PV.
In addition to grid-tied string inverters, the product range also includes hybrid and battery inverters for energy storage, accessories for grid management and operations and maintenance services. KACO new energy is a pioneer in the use of silicon carbide power transistors. From the advantage of silicon carbide's high thermal load capacity, the company has developed a range of PV string inverters with the leading efficiencies in the industry and has also been able to optimize them for use in particularly hot climates. Matched to these economical inverters and their topology with a single MPP tracker, the Virtual Central system design approach ensures savings on solar park investments.

More information at: https://kaco-newenergy.com/

About Fraunhofer ISE:

The Fraunhofer Institute for Solar Energy Systems ISE creates the technological foundations for supplying energy efficiently and on an environmentally sound basis in industrialized, threshold and developing countries. With its research focusing on energy conversion, energy efficiency, energy distribution and energy storage, it contributes to the broad application of new technology.
Fraunhofer ISE develops materials, components, systems and processes in five business areas. In addition to its R&D, the institute offers testing and certification procedures. Furthermore, it features an excellent laboratory infrastructure and is certified according to the quality management standard, DIN EN ISO 9001:2015. Founded in 1981, Fraunhofer ISE, with a staff of 1300, is the largest solar research institute in Europe.
In its work on Power Electronics, Grids and Smart Systems, Fraunhofer ISE mainly addresses research topics from the electricity sector. We are working on optimizing the interaction between efficient generation from renewable sources, a reliable supply for consumers, energy storage and stable operation of electricity grids. Furthermore, coupling between energy sectors, e. g. the transport or building sectors, represents another important aspect of our activities. Power electronics is becoming an increasingly important technology for the future energy supply.

More information at: https://www.ise.fraunhofer.de/en.html

Content

1 Introduction

Solar modules are generally operated at their maximum power point (MPP) on order to maximize their yield. Since the max. system voltage today is usually 1500 VDC, modules are first connected in series to utilize the voltage range for power scaling of the systems. For further scaling, the module strings are then connected in parallel to an inverter. The tracking of the point of maximum power is done by the inverter in system concepts with string inverters.
There are currently two different concepts for string inverters on the market. In single-stage inverters with single MPP tracking, all module strings connected to the inverter are connected in parallel. In this case, the inverter tracks the voltage to the point of maximum power resulting for the entire PV generator. However, as this can vary from string to string, mismatch losses can occur in this case.
The second concept pursued on the market consists of a two-stage concept, in which the first stage consists of several parallel DC-DC-stages. Up to 2 strings can be connected in parallel at each DC input in conventional designs. Each input can then independently adjust the input voltage, allowing for more small-scale MPP tracking. This approach can minimize voltage-related mismatch losses between module strings. The following figure shows both concepts as a block diagram.

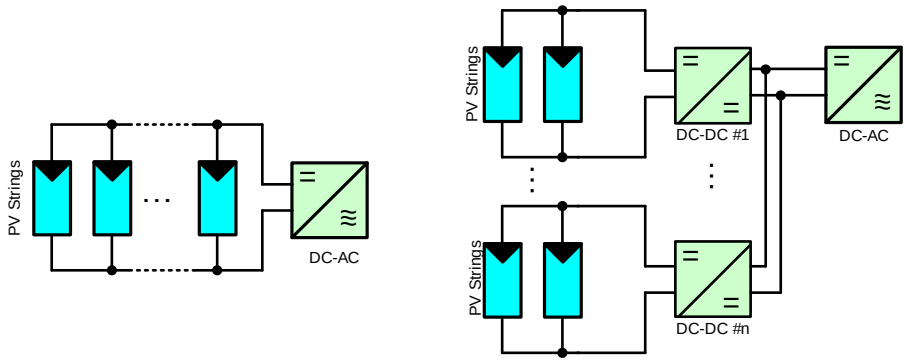

Figure 1: Block diagram of string inverters with single-MPPT (left) and multi-MPPT (right)

The question of whether and when the use of an inverter with multiple independent DC inputs is beneficial is analyzed comprehensively in this study. The focus of the study is on mismatch losses occurring between module strings. However, other effects such as input voltage range of the inverters, inverter efficiencies and the influence on the system design are also considered. The investigations are based on yield simulations with the PVSyst© software, provided that the corresponding effect can be reasonably represented in the software. For some of the effects, PVSyst© only allows a constant percentage loss calculation. In this case, own analytic and numeric calculations were performed to evaluate the effect.

The study was carried out on behalf of Kaco new energy GmbH.

2
Fundamentals and outline of study

PVSyst© is a widely used simulation software for yield calculations of PV plants. The plants can be modeled with a high level of detail. The simulation is then based on weather data for a given period. For the components used (modules and inverters), there is an extensive database with which models can be generated quickly and conveniently. However, PVSyst© excludes any liability for the accuracy of the data, as the model data is supplied by the respective manufacturers.
The PV module characteristics are modeled in PVSyst© using the single-diode model. Of course, the losses caused by mismatch also depend to a large extent on the accuracy of this modeling. Therefore, the accuracy of this model is first investigated and evaluated in the study (cf. chapter 3).

By default, PVSyst© uses weather data with a resolution of hourly values. Even though it is possible to integrate own weather data with higher resolution in the software, these data is then averaged into hourly values in the program and the simulation is then carried out with hourly values. In the past, it could be shown that the resolution of weather data has an influence on the optimal design of the inverter[1]. The influence of the resolution of the weather data on the simulation results is therefore investigated in more depth in chapter 4.

In chapter 5, the analysis of different effects which can lead to a mismatch between strings is carried out and the corresponding expected losses are furthermore quantified. For this purpose, different scenarios (plant type, location, etc.) are first defined for each of the mismatch effects for which the analysis is carried out. The following effects are addressed in the corresponding subchapters:

- Mismatch due to heterogenous string configuration
- Mismatch due to manufacturing tolerances of module parameters
- Mismatch losses due to temperature dispersion in the field
- Mismatch losses due to variation of module orientations and tilts
- Mismatch losses due to string cable length
- Near Shading losses
- Soiling losses
- Aging losses
- Mismatch losses due to moving clouds
- Effect on parameters of inverter (input voltage, efficiency, AC-voltage)

Chapter 6 contains an overall evaluation of the results and a summary thereof.

[1] Burger, Bruno, and R. Ruther. "Site-dependent system performance and optimal inverter sizing of grid-connected PV systems." *Conference Record of the Thirty-first IEEE Photovoltaic Specialists Conference, 2005.*. IEEE, 2005.

3
Part II: Model accuracy of single diode model for PV modules

3.1 Basics

The PV module characteristics in PVSyst© are modeled using a single-diode model. A detailed explanation of the model is given in the appendix. Based on the model parameters of the modules, PVSyst© generates corresponding I-V and I-P curves for different irradiances and temperatures and calculates the point of maximum power in each simulation step. In the past, the low-light behavior in particlular was not accurately represented by this model due to high series resistances in the modules. The two-diode model has achieved a higher accuracy in this case. To evaluate whether the model has sufficient accuracy for today's modules, curves were generated for a specific module (370 W mono-Si PERC) with the model used in PVSyst© and these were compared with measured values of the module. The measurements were carried out at Fraunhofer ISE in the CalLab[1].
The model parameters were first extracted from the PAN file provided by PVSyst©. However, in order to evaluate the model accuracy, a renewed parameter fit was performed using the real measured data and the results were compared.

3.2 Comparison of model and measurements

In the following graph, modeled curves based on the model parameters provided in PVSyst© (PAN file) are compared with the measured curves.

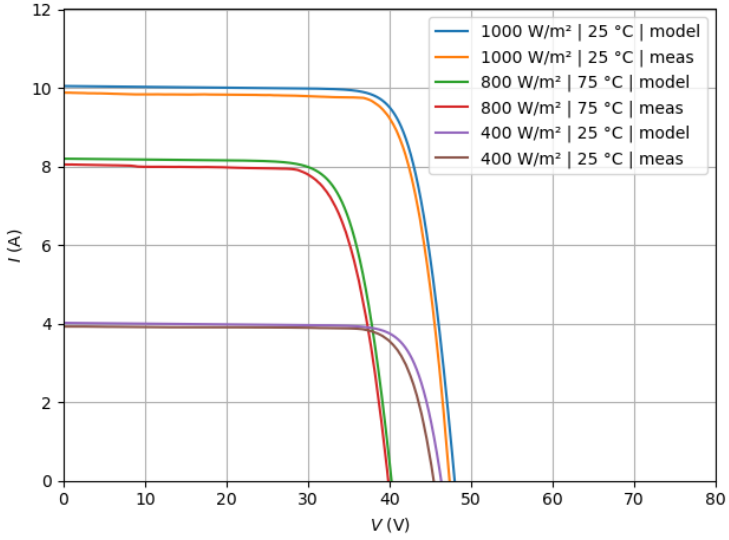

Figure 2: Comparison of the curves using the PAN file from PVSyst and the measured data for a single module with different irradiances and temperatures.

The performance of the module with the measured values deviates visibly downwards. If a new parameter fit for the module is performed based on the measured data and the modeled curves are then compared with the measurements, there is very good agreement between the model and the measurement (see Figure 3). The physical explanation that newer PV modules can be more accurately modeled by 1-diode models

[1] https://www.ise.fraunhofer.de/de/fue-infrastruktur/akkreditierte-labs/callab.html

than it used to be for older modules is that especially the recombination losses (both bulk and surface) have been reduced due to better materials and better surface passivation. The second diode in the 2-diode model usually models these recombination losses.

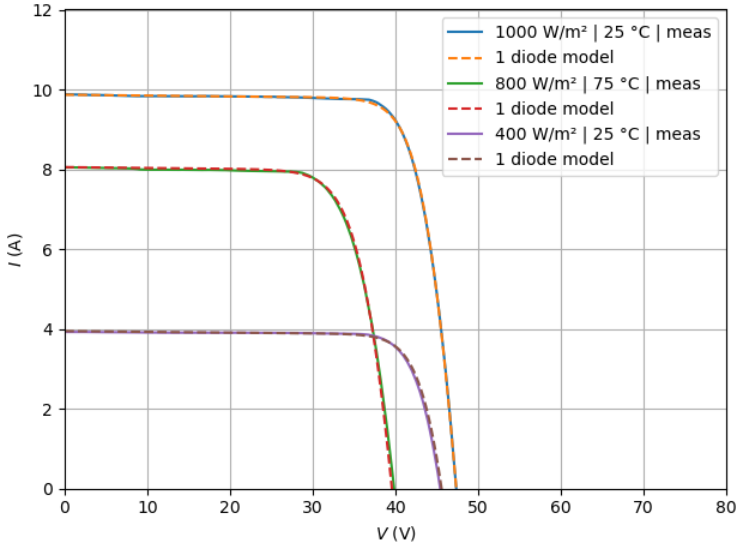

Figure 3: Comparison of the curves of the model (parameter fit based on measured data) and the measured data for different irradiances and temperatures.

The model and model parameters can therefore be used to determine V-I and P-I characteristics and the respective MPP for different irradiances and temperatures.
The accuracy depends largely on the accuracy of the model parameters used. The parameters stored in the PVSyst© database in the PAN file is provided from the manufacturer. PVSyst© only performs a plausibility check of the values. In order to have an independent data source for the highest possible accuracy in the yield simulation, it may be useful to carry out measurements in an independent certified laboratory. However, this deviation has qualitatively no influence on the simulation results performed in the study and does not as affect the fundamental results.

3.3 Results for Canadian Solar CS3W-410P 1500V

For the analysis in chapter 5, the module CS3W-410P 1500V from Canadian Solar is used. The parameters stored in the original PVSyst© database are used as model parameters. The basic data is summarized again in the following table.

Table 1: Specifications of CS3W-410P 1500V according to PAN File

Parameter		**Value**
Open Circuit Voltage	V_{OC}	47,6 V
Short Circuit Current	I_{Sc}	11,06 A
MPP Voltage	V_{MPP}	39,1 V
MPP Current	I_{MPPP}	10,49 A
Nominal Power	P	410 W

In the following, the resulting curves of the model for different irradiances and temperatures are plotted. Further curves can be found in appendix 3.3.

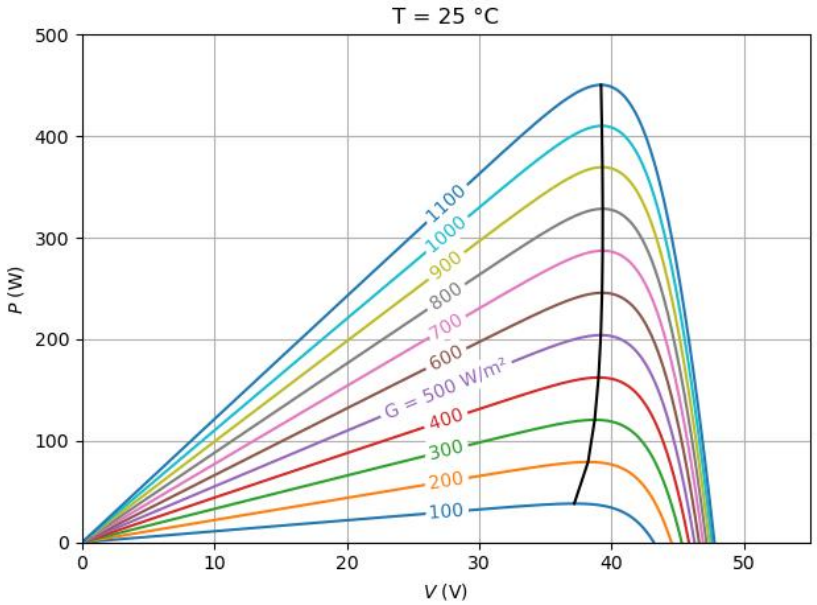

Figure 4: Modeled curves of the CS3W-410P 1500V for different irradiations and 25 °C

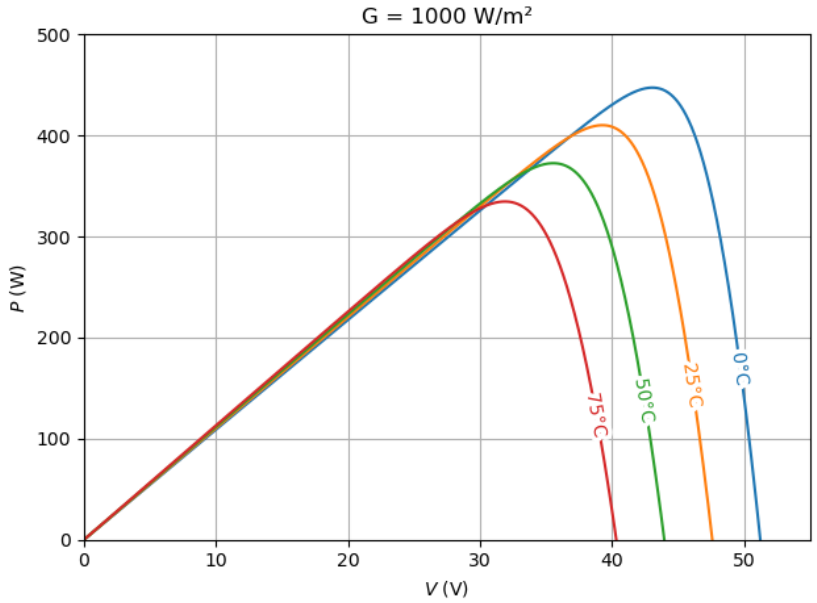

Figure 5: Modeled curves of CS3W-410P 1500V for different temperatures at constant irradiation of 1000 W/m².

Basically, one can observe that the MPP voltages change only very slightly with different irradiances. For varying temperature, the change is much more pronounced. In general, it can be deduced from this that mismatch effects that arise due to different irradiance, such as the combination of different orientations and installation angles, only lead to minor mismatch losses. Temperature gradients in the field, on the other hand, may have a larger effect.

4
Part I: Influence of time resolution of meteorological data

PVSyst© uses hourly average values for the meteorological data (solar irradiation, temperature, wind speed, etc.). Especially faster effects such as cloud-drifts or peaks in solar irradiation might be underestimated with the averaged values as for example the maximum power limit of the MPP tracker might be reached over a short period, but this limit might not be visible with the averaged meteorological data. The study conducted a small analysis of the yields for two different time steps of 15 min and 60 min.

4.1 Input data

The used meteo data set was measured at Fraunhofer ISE (48°00'38.2"N, 7°50'08.9"E) and this study uses the results of the year 2016. The elevation above sea level of most of the sensors is approximately 275 m. The 60 min dataset was generated by averaging the 15 min dataset. The used parameters for the simulations are summarized in Table 2.

Table 2: Meteo data used for the study

Parameter	Unit	Annotation
Sun azimuth	°	0° ≙ north, 90° ≙ east ..
Sun elevation	°	0° ≙ horizontal, 90° ≙ vertical
Horizontal irradiation	W/m²	
Diffuse irradiation	W/m²	
Direct normal irradiation	W/m²	
Ambient temperature	°C	

Figure 6 depicts the incident irradiation for a PV module oriented to the south with an elevation angle of 35°. It can be clearly seen that for a sunny day, the hourly averaged values are approximating the more precise 1 min values very good. However, the minima and maxima are not represented in very well for a cloudy day. The following simulations will investigate how this behavior affects the overall yield results.

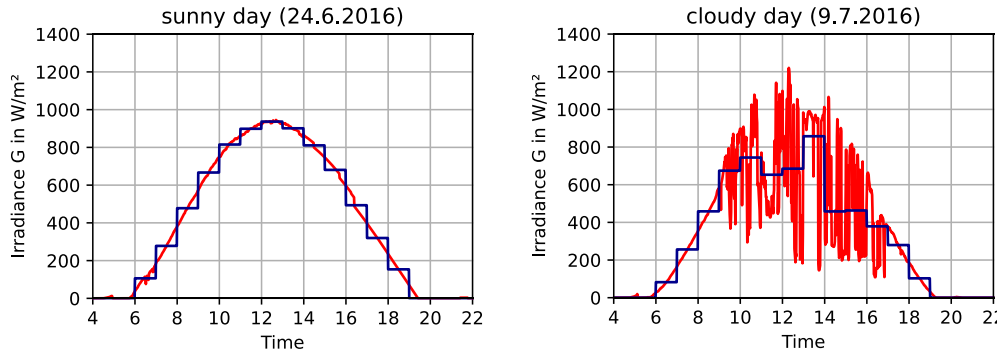

Figure 6: Comparison of 1 min irradiation values with 1 hour averaged values for a sunny and a cloudy day

4.2 Model

The PV modules were simulated with the 1-diode model which is described in detail in the appendix. Two different string layouts were simulated:

1) 8 strings of 18 modules (CS3W-410P 1500V)
2) 8 strings of 20 modules (CS3W-410P 1500V)

The simulations were performed for an orientation to the south with 35° elevation.

The incident irradiation is calculated for each time step according to the metrological data. The ambient temperature and the irradiation are then used to estimate the cell temperature. With the irradiation and the cell temperature, the 1-diode model is solved, and the resulting IV curve is used to determine the MPP point as well as possible losses, which occur due to inverter limitations.

The theoretical available energy at the MPP over the whole simulation period is represented by E_{mpp}. The inverter has a minimum power (120 W in this simulation) to start operation. All losses due to the minimum power requirement of the inverter are summed up in the variable $E_{loss,Pmin}$. In a similar manner, all losses which occur if the available power at the MPP of the string exceeds the 60 kW limitation of the MPP tracker are aggregated in the variable $E_{loss,Pmax}$. $E_{loss,Vmax}$ signifies the occurring losses due to the maximum voltage limitation of the MPP tracker (900 V for this study) and $E_{loss,Vmin}$ the losses which occur if the MPP cannot be tracked any longer due to the minimum voltage limitation of the MPP tracker (580 V).

4.3 Results

Table 3 summarizes the cumulative results for the yield simulations. It can be observed that the losses due to the maximum power limitation increase with smaller timesteps. This can be explained because with longer periods of averaging, peaks in the irradiation are filtered out (low-pass effect). All other losses stay very small for the investigated simulations.

timestep (min)	String length	E_{mpp} (MWh)	$E_{loss,Pmax}$ (kWh)	$E_{loss,Pmin}$ (kWh)	$E_{loss,Vmax}$ (kWh)	$E_{loss,Vmin}$ (kWh)
15	18	72.45	3.86	5.66	0	1.02
60	18	71.65	0	6.28	0	1.08
15	20	80.5	363.45	5.3	0	0.77
60	20	79.61	165.37	5.41	0	0.85

Table 3: Loss distribution for simulations with different timesteps and different string lengths

Figure 7 and
Figure ***8*** depict the histograms of the MPP voltages for a simulation with a timestep of 60 min or 15 min respectively. It can be observed that the distribution gets smoother and more distributed to lower and higher voltages. Similar histograms are shown in Figure 9 and

Figure ***10*** for the distribution of the MPP power. A smoothening effect can be observed as well. In addition, the almost linear decrease for power above approx. 60 kW is more clearly visible.

A clear difference in the histograms both for the MPP voltages and the MPP power can be observed, however, as summarized in Table 3, the overall effects for a yield simulation for typical string layouts are rather small. In the scenario with a string length of 20 modules, a difference of approx. 200 kWh could be observed, which is in the range of 0.25% of the overall yield.
Losses resulting from falling below the minimum MPP voltage can be neglected for all cases. They amount to only max. 1 kWh in all cases.

The histograms for the simulations with the string length of 18 modules are depicted in appendix.

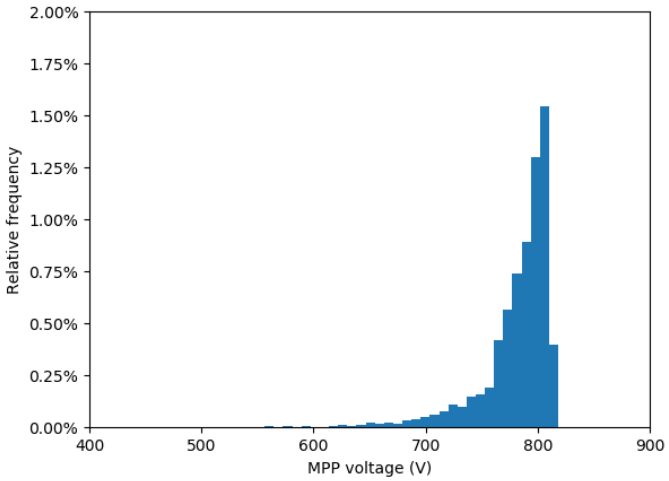

Figure 7: Histogram for the distribution of the MPP voltages in the year 2016 for a string with 20 modules and 60 min timesteps.

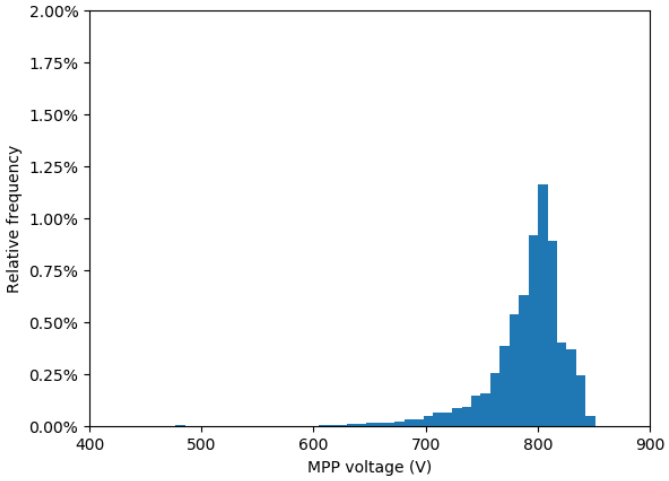

Figure 8: Histogram for the distribution of the MPP voltages in the year 2016 for a string with 20 modules and 15 min timesteps.

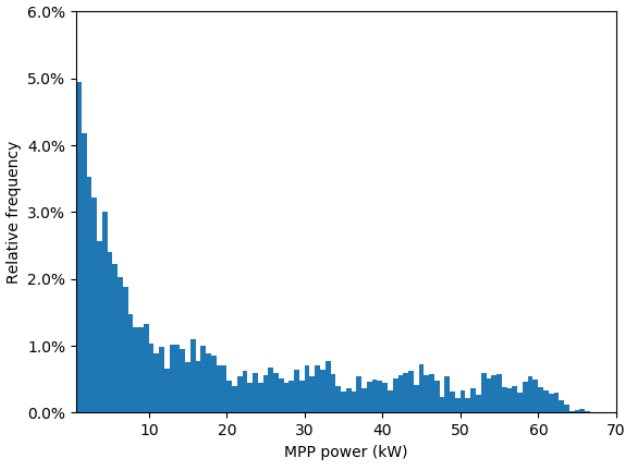

Figure 9: Histogram for the distribution of the MPP power in the year 2016 for a string with 20 modules and 60 min timesteps.

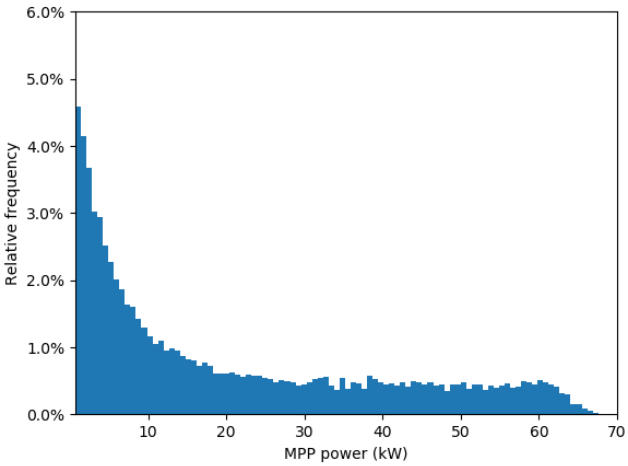

Figure 10: Histogram for the distribution of the MPP power in the year 2016 for a string with 20 modules and 15 min timesteps.

4.4 Influence of the resolution of the weather data on shading effects

In chapter 5.7, various shading effects are simulated with PVSyst© and the additional yield from multi-MPPT inverters is estimated. The simulations are carried out on an hourly basis (finest possible resolution in PVSyst©).
Depending on the location, different shading diagrams result. These are shown in Figure 50 (Arkona) and

Figure 51 (Abu Dhabi) in the appendix. Especially at sunrise and sunset the highest rates of change of the sun angle per time occur. In Abu Dhabi this change is even larger than in Arkona. The hourly resolution inevitably leads to inaccuracies here, since the shading situation already changes considerably within one hour. In case of southward orientations and tracker systems along the north-south axis (cf. chapter 5.7), this effect is compensated during the day as long as the shading scenery is symmetrical in the morning and in the evening. For the cases outlined, the simulations carried out in chapter 5.7 lead to meaningful results. For asymmetrical shading scenarios during the day, however, a simulation with a higher time resolution would be useful for estimating the yield.

5
Impact on annual plant yield for different cases

5.1 Basics /Scenarios

For the investigations, two basic types of plants were distinguished and modeled. Scenario A is designed as a rooftop system with an inverter size of 60 kVA. Scenario B is a design for ground-mounted systems based on a string inverter with 165 kVA. Two representative locations were chosen: Arkona, Germany (AK) and Abu Dhabi, United Arab Emirates (AD). The following table summarizes the basic framework conditions.

Table 4: Framework for Scenario A und B

Parameter	Scenario A	Scenario B
Plant Type	Rooftop	Ground-mounted
Inverter Power	60 kVA	165 kVA
Inverter	Kaco blueplanet 60	Kaco blueplanet 165
P_{DC}/P_{AC} ratio	1	1
Number of MPPTs	1 (6)	1 (9)
PV Module	CS3W-410P 1500V	
Max. PV Generator voltage	1000 V	1500 V
Number of Modules per String	18	AK: 28 AD: 29
Number of Strings	8	15 (16)
Orientation	South	
Optimal Tilt	AK: 40° AD: 22°	
Tracker System	-	(Single Axis NS)

The selection of the optimal installation angle (tilt) was calculated by optimizing the annual yield in PVSyst based on a typical meteorological year. The calculated optimization curve can be found in Appendix 5.1. The determined tilt agrees with the values of the Global Solar Atlas[1]. Depending on the weather data used and the optimization goal of the plant, there may be deviations in the angle. However, this has no effect on the fundamental results in this study.

For the modeling, real inverter data from two inverters of Kaco New Energy GmbH are used for the single MPPT configuration. Variants with multiple MPPTs were synthetically generated from these inverters. The inverter efficiency was assumed to be constant in each case. In the following comparisons of different configurations, the efficiency losses of the inverter were not taken into account (cf. chapter 5.11).

However, as the reliability of the efficiency data in PVSyst© in general is questionable (cf. chapter 5.11) the yield estimation is done without considering efficiency losses of the inverter as mentioned before. In PVSyst© this amount of energy is referred to as "Virtual energy at PV array". All simulation results leading to a yield gain by the integration of multi MPPT inverters can therefore be understood as a maximum yield gain. When taking

[1] https://globalsolaratlas.info

the efficiency of real inverters into account, this value will probably be reduced as the efficiency of multi MPPT inverters can be assumed to be lower than the efficiencies of single stage inverters.

Impact on annual plant yield for different cases

Simulation parameters

The following table summarizes the parameter set in PVSyst© for the simulations.

Table 5: Simulation parameters

Parameter	Value	Comment
Const. Thermal loss factor	29 W/m²K	PVSyst© default
Thermal Corr. Factor related to wind	0 W/m²K	Not considered
Ohmic DC losses	1.5 %	PVSyst© default
Ohmic AC losses	0 %	Not relevant for analysis
Light Induced Degradation	2 %	PVSyst© default
Power quality of modules	0 %	Not relevant for analysis
Mismatch losses of modules	0 %	Analyzed separately in Chapter 5
Mismatch in strings	0 %	Analyzed separately in Chapter 5
Yearly soiling loss	0 %	Not relevant for analysis
IAM losses	s. PAN	According to module data
Auxiallary losses	0 W	Not relevant for analysis
Aging	0 %	Discussed separately in Chapter 5
Non availability	0 %	Not relevant for analysis
Spectral correction	No	Not relevant for analysis

Meteorological data for PVSyst© simulations

Meteonorm is a common data source for PV system yield simulations and provides easy access to a typical meteorological year (TMY) resolved in hourly values. The weather data used was TMY data from Meteonorm 8.0 for the two sites. Other data sources would quantitatively influence the simulations. However, fundamental changes in the conclusions with other weather data sources are not expected. The influence of the resolution is discussed in detail in chapter 4.

5.2 Mismatch due to heterogenous string configuration

In most cases, only strings with the same number of modules are connected in parallel during system planning. However, especially for smaller systems, it can make sense to combine different string lengths. Of course, this inevitably leads to mismatch losses in inverters with single MPPT. In the following, these will be quantified for different configurations. These investigations refer to variants of scenario A at the Arkona site. For this purpose, different combinations of strings with 18 and 19 modules in series were considered in each case. Since PVSyst© does not offer the possibility of connecting different string lengths in parallel at one MPPT or inverter input, parameters for each of the configurations were generated synthetically. To do this, the resulting characteristic

curve of the entire generator was generated for each case using the single-diode model. From these curves, a parameter fit was then used to generate the synthetic parameters for one module with the corresponding values for a homogeneous string configuration with 18 modules. The main changes in this case are open circuit and MPP voltage.
In the following a curve for the configuration 4x 18 + 4x 19 is shown. Table 6 shows the parameters determined for all combinations. The curves of the other cases can be found in the appendix.

Impact on annual plant yield for different cases

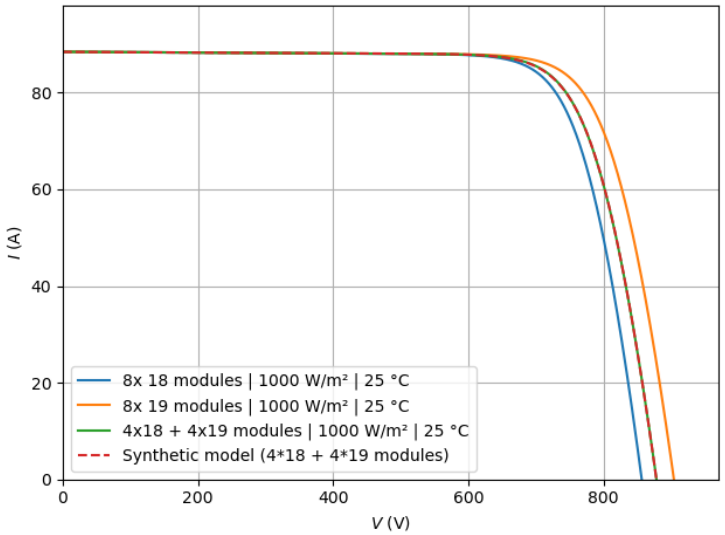

Figure 11: Synthetically generated characteristic curve for the combination 4x 18 + 4x 19

String configuration	V_{OC}	V_{MPP}	I_{Sc}	I_{MPPP}
1: 8x 18 + 0x 19	47.600	39.261	11.060	10.448
2: 7x 18 + 1x 19	47.879	39.436	11.058	10.443
3: 6x 18 + 2x 19	48.173	39.631	11.057	10.438
4: 5x 18 + 3x 19	48.482	39.847	11.056	10.434
5: 4x 18 + 4x 19	48.806	40.095	11.056	10.430
6: 3x 18 + 5x 19	49.145	40.375	11.056	10.429
7: 2x 18 + 6x 19	49.498	40.686	11.057	10.431
8: 1x 18 + 7x 19	49.865	41.040	11.058	10.437
9: 0x 18 + 8x 19	50.244	41.441	11.060	10.449

Table 6: Specification of corresponding synthetic module for different configurations

Yield simulations for scenario A in Arkona were then carried out in PVSyst© using the synthetic module parameters. This was done for each case with single MPPT, with 4 MPPTs and 6 MPPTs. In the following graph, the relative annual additional yield for these cases is plotted. The largest mismatch losses occur with a 50/50 configuration of the PV generator amounting to 1.05 % for single-MMPT. For asymmetric configurations, the mismatch decreases. For the case of an inverter with 4 MPPTs, mismatch occurs for odd ratios between the string lengths, since in this case one string with 18 and one string with 19 modules are always connected in parallel at one of the MPPTs. The mismatch here is ~0.26% in each case.
The results show that even with the artificially created and expected mismatch in this case, the yield losses are still relatively low with single-MPPT. A corresponding simulation for scenario B was not carried out since the results can be transferred accordingly.

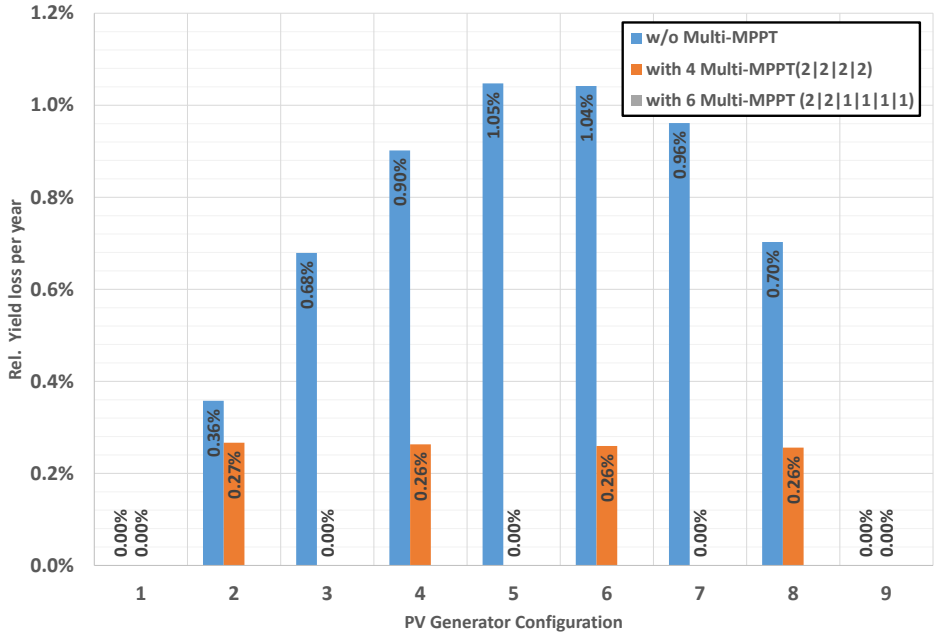

Impact on annual plant yield for different cases

Figure 12: Relative yield loss with different configurations of PV generator and different number of MPPTs (1 ,4 ,6).

5.3 Mismatch due to manufacturing tolerances of module parameters

In order to minimize mismatch losses, today's solar modules are sorted very precisely with regard to the production-related parameter scatter. This leads to the fact that there are up to 6 power classes in 5 W steps per module type of a manufacturer. However, a residual tolerance remains with regard to the parameters of the module. In many data sheets there is no information about this, mostly only a positive power tolerance of e.g. +10 W is given for the CS3W-410P 1500V. For the consideration of mismatch losses, however, it makes sense to specify the tolerance separately for voltage and current of the module. Some manufacturers specify this, usually values smaller than 3 % are mentioned here (e.g. REC Solar Holdings AS). Therefore, a tolerance of 3 % was used for the following calculations, since this can be regarded as the absolute worst case.
In order to make an analysis of the resulting mismatch losses with this information, the deviation in current and voltage must be considered independently of each other, since the deviations have different effects. If a normal distribution for current and voltage is applied to the solar generator from scenario A (8 strings of 18 modules each) for each of the 144 modules installed, the following picture emerges. In each string, the current that can be delivered is determined by the module with the lowest current. A downward deviation of a module current therefore immediately leads to a mismatch. This current-induced mismatch cannot be compensated by MPPT trackers on string level, instead module integrated optimizers would be necessary.
Looking at the variance of the voltage, the picture is different at string level, since the string voltage is formed from the sum of the individual voltages. Depending on the length of the string, it is therefore to be expected that the tolerance over a string is lower than the tolerance of an individual module.
PVSyst© provides a tool for statistical analysis of this effect. The tolerances for voltage and current can be set separately, so that the two effects can be easily considered separately. The following figure shows a resulting generator curve for Scenario A with 0 % tolerance for current and 3 % tolerance for voltage. PVSyst© calculates the mismatch between this characteristic curve and the characteristic curve with exact datasheet values.

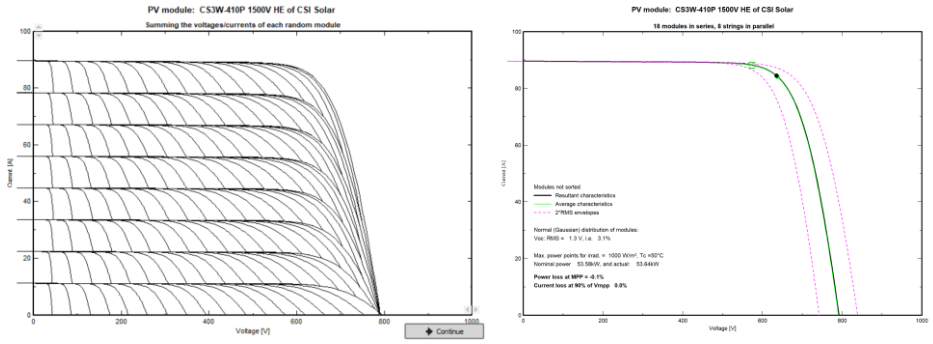

Figure 13: PV generator characteristic curve for scenario A with statistical normal distribution of Voc and 3 % deviation (left) - Resulting characteristic curve of the generator and comparison to the characteristic curve without tolerance (right)

This procedure is repeated to obtain a histogram of mismatch losses with statistical significance. From this histogram, one can then determine the mean deviation to quantify the effect. The histogram for the evaluation of 440 generated characteristic curves is shown below. The mean losses in the MPP are less than 0.1 % and thus negligible. For larger generator voltages (scenario B), an even smaller value results, since the number of modules increases. A higher variance of the voltage would also lead to higher losses, but calculations have shown that even with a tolerance of 10 %, only an average deviation of 0.3 % would result in the configuration.
If the current of a module is assigned with a corresponding tolerance, this quickly leads to relevant mismatch losses. With 3% tolerance, the same configuration results in 0.8 % mean losses. The corresponding curves are shown in the appendix.

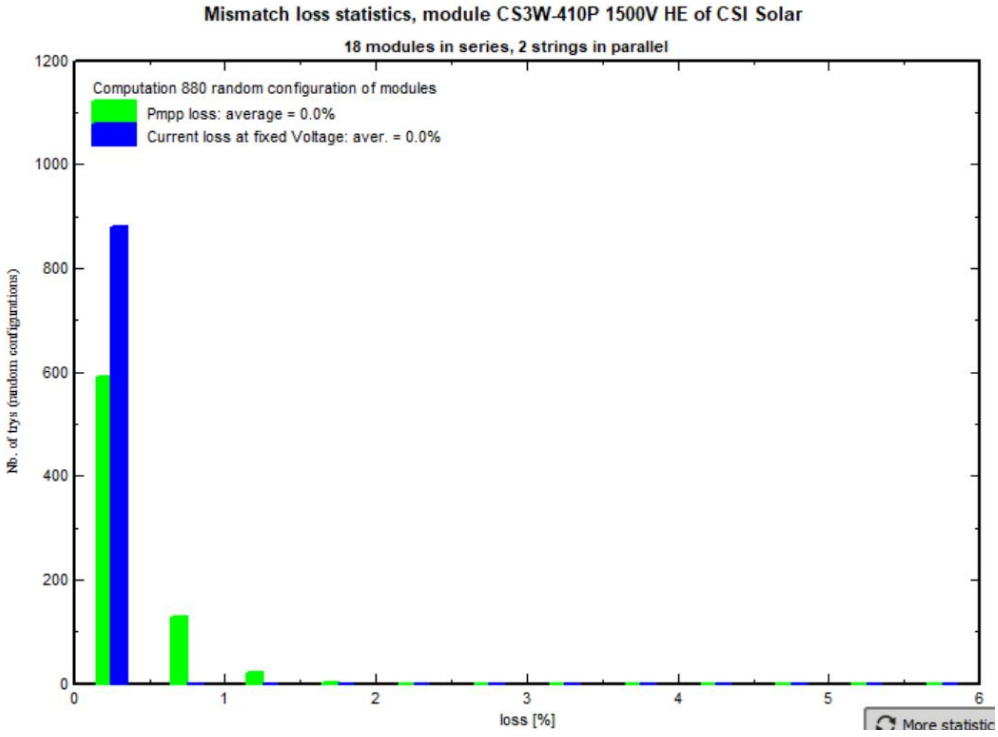

Figure 14: Histogram for 440 random arrangement in scenario A with a tolerance of 3 % in voltage

5.4 Mismatch losses due to string cable length

In most cases, the length of the connecting lines of the strings to the inverter have different lengths. In theory, this leads to different voltage drops across the lines and thus also to mismatch between the strings. In the following, the resulting losses will be estimated for two scenarios. For this purpose, realistic plant designs were made for each case and the maximum string length difference was estimated. The two cases are outlined in the following table.

PVSyst© allows the estimation of mismatch losses in the MPP between two strings with different connection lengths. This tool was used to estimate these losses for both scenarios. However, since this estimation is the mismatch between the two extremes, the average value for the entire generator is significantly lower. Likewise, operating points over the year below the minimum MPP lead to a further reduction of the value for the entire plant yield, so that this effect can be neglected for both scenarios investigated.
The detailed results of the calculation from PVSyst© can be found in the appendix.

Impact on annual plant yield for different cases

Table 7: Framework for Scenario A and B

Parameter	Scenario A	Scenario B
P_{DC}/P_{AC}	1.2	1.4
Number of Strings	10	20
Number of Rows	5	10
Strings per row	2	2
Pitch between rows	4 m	4m
Size of PVGenerator	20 m x 80 m	50 m x 120 m
Estimation of string cable length	60 m	120 m
String cable diameter	4 mm² (Copper)	
Mismatch @ ΔT = 2.5K between two strings	0.03 %	0.05 %

5.5 Mismatch losses due to temperature dispersion in the field

As mentioned before, a heterogeneous temperature distribution in the generator can lead to mismatch losses. The temperature distribution depends on various factors (wind, wind direction, geometry of the plant, orientation of the plant, topography of the terrain, module technology, etc.) and is therefore not trivial. In literature, a spread of 1 K is sometimes estimated per 100 modules[1]. For a plant in Portugal one can find detailed measurement data over one year. In this plant temperature differences of up to 10 K were measured[2]. From the authors' point of view, these measurements can be regarded as a worst-case scenario. On the one hand the location has very little wind, on the other hand the arrangement of the modules on the tracker table is unusually high (8 module rows). The measurements have shown that the largest deviations exist in the vertical direction. It can therefore be assumed that with today's installation with 4 rows per table (fixed elevation) and 2 rows (with tracker) smaller temperature differences occur. PVSyst© allows the estimation of the mismatch between two strings operating at different temperatures. From the authors' point of view, it would be unrealistic to perform the calculations with 5 K or 10 K, as these are rather to be considered as maximum values. In order to obtain a constant loss factor for the whole plant, the calculation with 2.5 K is to be considered as a realistic average value for different plant configurations and

[1] Dirnberger, Daniela, et al. "Uncertainty of field IV-curve measurements in large scale PV-systems." *Proceedings of the 25th European Photovoltaic Solar Energy Corference and Exhibition* (2010): 4587-4594.

[2] Escribano, Mikel Muñoz, et al. "Module temperature dispersion within a large PV array: Observations at the amareleja PV plant." *IEEE Journal of Photovoltaics* 8.6 (2018): 1725-1731.

locations. In the following, results of calculations in MPP between two strings are shown. In both cases, only small losses of 0.06 % /or 0.05 % are obtained. The detailed curves for these results can be found in the appendix.

Impact on annual plant yield for different cases

Table 8: Simulated losses when connecting 2 strings in parallel with 2.5 K temperature difference in MPP

Parameter	Scenario A	Scenario B
Max. Delta T	2.5 K	
T of strings	40 °C / 43 °C	
VMPP of string 1	665.2 V	1034.8 V
VMPP of string 2	657.1 V	1024.2
P of string 1	6975.3	10850.4 W
P of string 2	6892.5	10743.2 W
Absolute power loss	4 W	5.6 W
Relative power loss	0.06 %	0.05 %

5.6 Mismatch losses due to variation of module orientations and tilts

Different Orientations

Particularly at locations in Germany, it has nowadays become attractive not to design systems facing south, but to plan a PV generator in which strings with an east and west orientation are combined in order to minimize the curtailment losses at outputs greater than 70 % of the nominal module power. For scenario A, various configurations were simulated using PVSyst© to calculate how much additional yield can be achieved by using a multi-MPPT inverter. The simulations were made for the Arkona site and for Abu Dhabi. The tilt angle for the east-west orientation was chosen to be 20° in both cases. For all configurations, the additional yield is less than 0.1 %. The location has a slight influence on the mismatch. In locations with more direct sunlight (Abu Dhabi) the mismatch is more noticeable. The additional yield here would be + 0.02 % points compared to a plant in Arkona.
A steeper installation angle leads to larger mismatch losses. However, simulations have shown that even at an angle of 40 °, the yield gains of multi-MPPT inverter increase on average by only about 0.01 percentage points.
In order to consider the influence of deviation from the optimal south orientation, simulations were performed with deviations of 2° and 10° with 50-50 splitting of the generator in each case. In these cases, the mismatch in the simulation is zero. The following table summarizes the results once again. Details of the simulations carried out for the variants can be found in the appendix.

Impact on annual plant yield for different cases

Orientation	String Layout	P_{DC}/P_{AC}	Location	Yield Gain
East-West	E: 5 / W: 5	1.2	AR	0.07 %
East-West	E: 5 / W: 5	1.2	AD	0.07 %
East-West	E: 4 / W: 4	1	AR	0.07 %
East-West	E: 4 / W: 4	1	AD	0.07 %
East-West	E: 1 / W: 9	1.2	AR	0.01 %
East-West	E: 1 / W: 9	1.2	AD	0.02 %
S: +2° / -2°	+2°: 5 / -2°: 5	1	AR	0.00 %
S: +10° / -10°	+10°: 5 / -10°: 5	1	AR	0.01 %

Table 9: Simulated yield gains from multi-MPPT for different PV generator configurations for Scenario A.

Different Tilts

Since in reality the tilt of different rows ist not exactly identical, this effect was also represented in the simulation environment for scenario A. The orientation of the PV generator in this case was to the south for both locations. However, the strings in the generator were each subjected to different deviations in the 50-50 distribution. In this case, even extreme deviations of 20° only result in possible yield gains of max. 0.01 %. The following table summarizes the results. Details of the simulations carried out for the variants can be found in the appendix.

Tilt	String Layout	P_{DC}/P_{AC}	Location	Yield Gain
35° / 45°	35°: 4 / 45°: 4	1	AR	0.00 %
20° / 30°	20°: 4 / 30°: 4	1	AD	0.01 %
20° / 40°	20°: 4 / 40°: 4	1	AR	0.01 %
15° / 35°	15°: 4 / 35°: 4	1	AD	0.01 %

Table 10: Simulated yield gains from multi-MPPT for different PV generator configurations for Scenario A with variation of tilts within the generator.

5.7 Near Shading losses

Near shading by a tree

To consider this effect, a representative shading scenario was defined in PVSyst©. For this purpose, the generator was defined as a coherent surface on a rooftop with a fixed installation angle of 40° (AK) or 22° (AD), so that the only shading that occurs is caused by the tree or another comparable obstacle. The following figure shows the shading scenario. The connection of the strings to MPPTs can be found in the appendix.

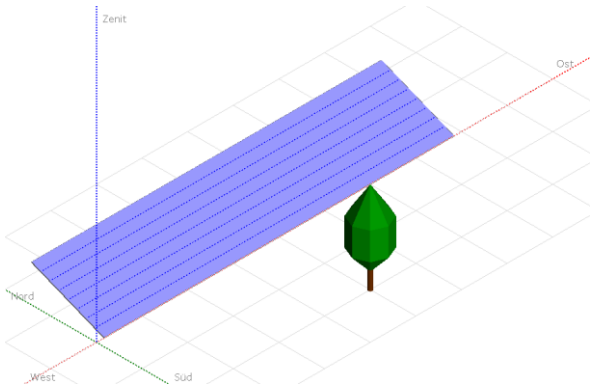

Figure 15: Shading scene with a tree for scenario A

The scenario was simulated with single and multi-MPPT inverters. At the Arkona site, the additional yield through multi-MPPT amounts to 1.0 %, the same value was found for Abu Dhabi. For these calculations, losses due to inverter efficiency were not considered. More details on the simulation conditions can be found in the appendix.

Table 11: Simulated yield gains from multi-MPPT for the shading scenario by a tree outlined above.

Location	Yield with Single MPPT *MWh/year*	Yield with Multi MPPT *MWh/year*	Relative Yield Gain
AK	68.853	69.560	1.0 %
AD	108.400	109.470	1.0 %

Near shading by module tables for PV generator with fixed tilt

In ground-mounted systems, the tilt of the module rows inevitably leads to shading for certain sun angles. To analyze this effect, different configurations were defined on the basis of scenario B and the additional yield was determined by multi-MPPT. The PV generator design was based on PV tables with 4 horizontal rows of 28 modules each (collector height per table: 4.2 m). The last table has only 3 module rows due to the total number of strings. The installation angle and orientation were chosen to be optimal for both orientations. Simulations with two different values for the row spacing were then performed for both locations and the potential additional yield was determined for multi-MPPT. The optimal row spacing was specified so that just no shading of the rows among each other occurs at noon on the shortest day of the year. In the second variant, the determined distance was halved. In the following figure the row configuration is sketched. In the following table the simulated row distances are described. Further details on the simulations can be found in the appendix.

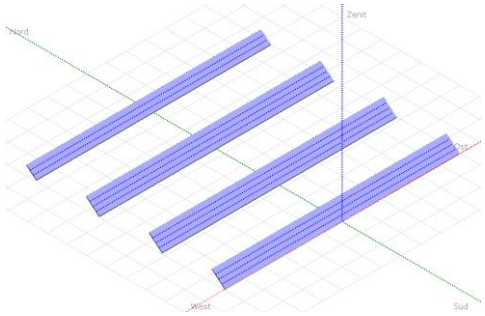

Figure 16: Shading scene row shadowing for Arkona (16m)

Location	Optimal row spacing	Reduced row spacing
AK	16 m	8 m
AD	6m	5m

Table 12: Optimized and reduced row spacing for both locations.

The results show that with an optimal row spacing, only very small mismatch losses occur due to shading. The closer the row spacing is selected, the greater the effect is. Particularly at the Abu Dhabi location, due to the greater proximity to the equator and the high proportion of direct sunlight, the reduction of the row spacing from 6 m to 5 m already leads to an increase of the voltage-induced mismatch losses by 0.33 % points. The following graph also shows that only a very small part of the losses caused by the additional shading are compensated by multi-MPPT. The overall yield reduction is 5.5 % for Arkona and 5.6 % for Abu Dhabi.

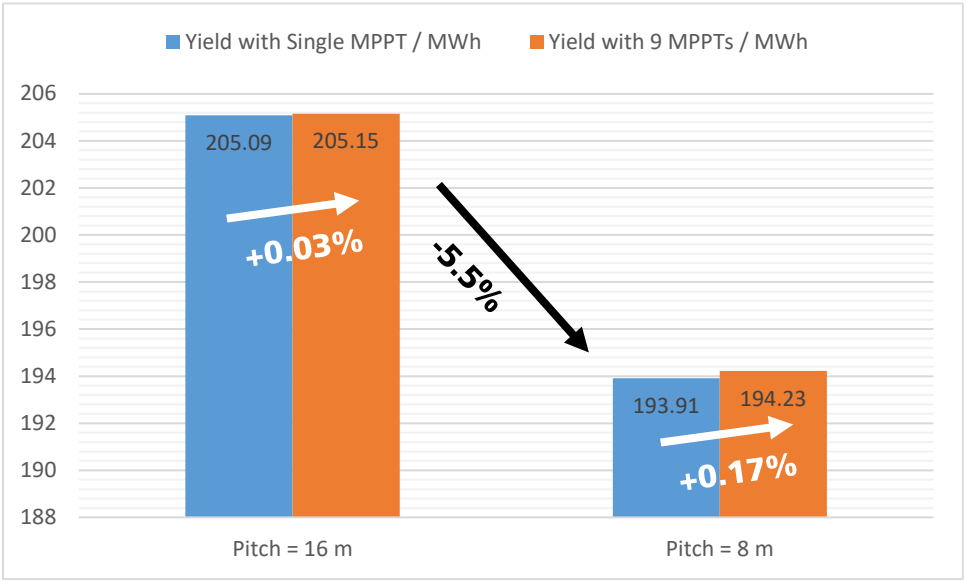

Figure 17: Simulation results with variation of row spacing for Arkona.

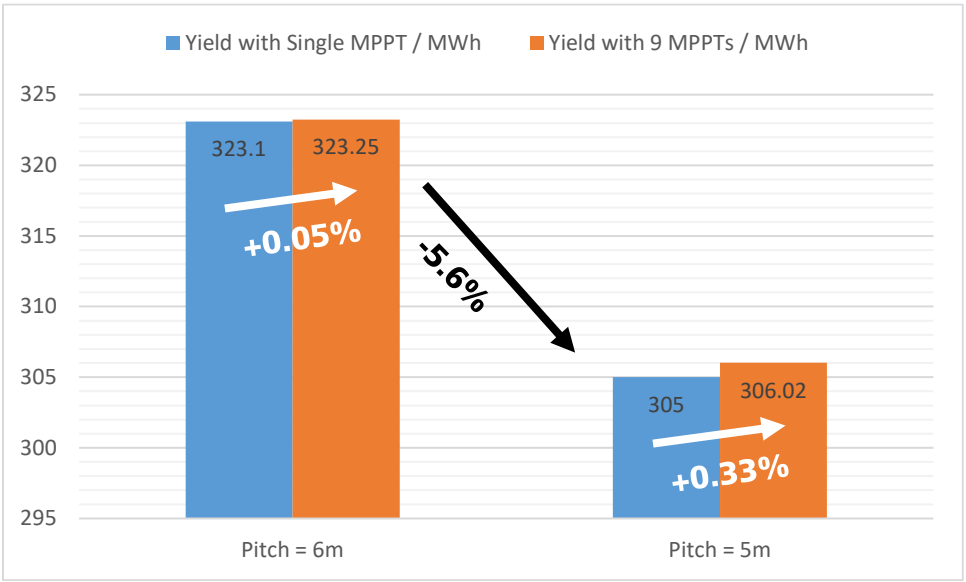

Figure 18: **Simulation results with variation of row spacing for Abu Dhabi.**

Impact on annual plant yield for different cases

Near shading by module tables for PV generator with single axis tracker (N-S)

The same considerations were made for PV generators with single axis tracking. The tracker system was defined as a single-axis tracking along the north-south axis. For each tracker, 2 module rows with 28 modules each were designed. For symmetry reasons, the number of strings was increased from 15 to 16, resulting in 8 identical trackers. To evaluate the shading effect, different distances were simulated for both locations. The basic scenario for a distance of 10 m is shown in the following figure. Further details of the models can be found in the appendix.

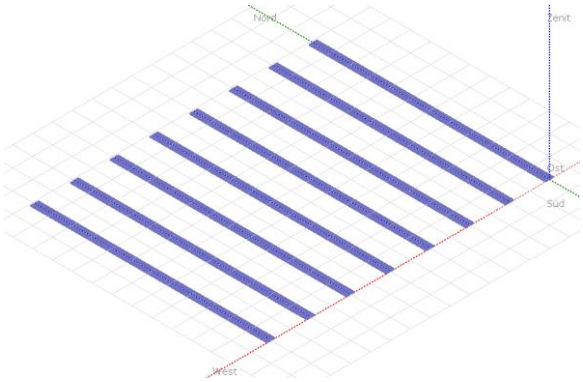

Figure 19: Shading scene tracker system (10m pitch between tracker)

Location	Max. pitch	Medium pitch	Min. pitch
AK	10 m	7 m	5 m
AD	5 m	4 m	3 m

Table 13: Simulated row spacing for both locations.

The picture is the same for all cases: only a very small part of the yield losses due to shading can be compensated by multi-MPPT at string level. Even with a spacing of 5 m between the trackers, multi-MPPT only results in an additional yield of 0.19 % in Arkona and 0.24 % in Abu Dhabi.
For plants optimized for yield per kW_p with larger row spacing, the additional yield can be neglected. Even with narrower row spacing with optimization in terms of yield per area, the additional yield is less than 0.25 % points. However, considering lack of reliable inverter efficiency data (see chapter 5.11), it is questionable whether this would lead to an additional yield in reality.

Impact on annual plant yield for different cases

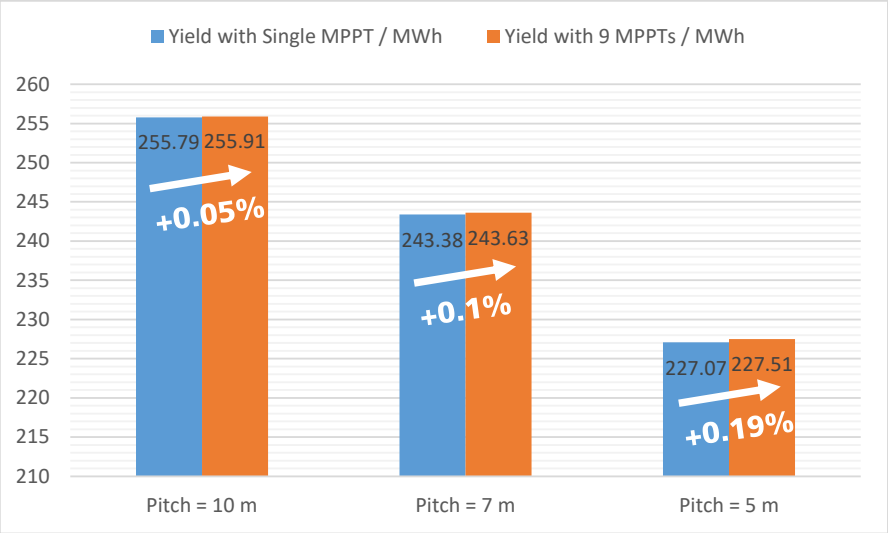

Figure 20: Simulation results with variation of the distance between the trackers for Arkona

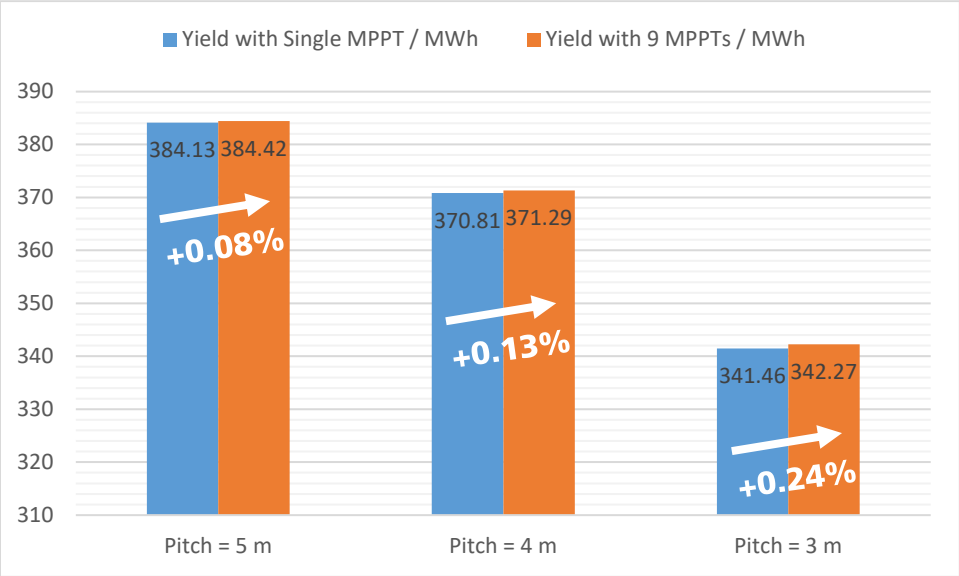

Figure 21: Simulation results with variation of the distance between the trackers for Abu Dhabi

5.8 Soiling losses

PVSyst© allows the simulation of soiling effects via a constant annual relative loss factor in percent. The losses are thus deducted as a generalized sum from the theoretical yield of the PV generator. In this way, simulative homogeneous pollution effects (e.g. dust) that affect the entire generator equally are considered. The use of multi-MPPT inverters would not lead to any additional yield in this case. However local pollution can hypothetically lead to mismatch losses between strings which can be compensated by multi-MPPT. However, these effects are very specific and, in the authors' view, can be neglected in relation to the other effects studied. This effect was therefore not considered further in the study.
In practice, inhomogeneous contamination or plant growth can lead to hotspots, which in turn affect the performance of the system.

5.9 Aging losses

Aging of PV modules leads to a degradation of the performance values of the modules over their lifetime. The extent of this effect depends strongly on the module technology

used. For the module type examined in the study, the authors consider an average annual degradation from 0.25 % to 0.55 % to be realistic. The degradation occurs stochastically over the entire generator. Similar to chapter 5.2, this effect becomes statistically uniform across the strings when reduced to the voltage of the modules. The average string voltage decreases by 0.55 % over the years. The mismatch between strings, however, increases to a significantly reduced extent. From the results of chapter 5.2 it can be concluded that this effect can be neglected in terms of additional yield for the selected module type.

Impact on annual plant yield for different cases

A separate effect is the reduced system voltage over the lifetime of the system. However, for the module technology considered, it could be shown in the simulation that with an annual aging of 0.55 %, the yield losses induced by the voltage limit after 25 years (in the 25th year) are only 0.1 %.

In the case of other module technologies with greater aging effects, a significantly greater additional yield can be achieved by multi-MPPT. In the investigations for the present study, however, the focus was placed on crystalline Si modules.

5.10 Mismatch losses due to moving clouds

Passing clouds lead to temporary inhomogeneous irradiance conditions over the PV generator. In general, it can be assumed that the effective irradiance can be reduced by up to 2/3 in the affected area. As already shown in chapter 3.3, the resulting mismatch is very small, since the MPP voltage changes only marginally over a wide range of irradiances (cf. Figure 4). In addition, this effect only occurs over a short period of time, depending on the wind strength. From the authors' point of view, this effect can therefore be neglected and was not investigated further.

5.11 Effect on parameters of inverter (input voltage, efficiency, AC-voltage)

In the previous investigations, the inverter characteristics were not considered in detail. The simulated additional yields are therefore to be understood as a theoretical maximum value that is possible when using multi-MPPT inverters. However, the characteristics of single MPPT and multi-MPPT inverters generally differ. Therefore, two of the properties relevant to the consideration of the effect are discussed below.

Voltage threshold of inverter

To be able to feed current from a DC voltage into a grid with a given AC voltage using a transformerless, single-stage inverter, the DC voltage must be above a minimum value. The following table shows the formulas and the values for different grids and for feeding in with and without the third harmonic. In the formula, efficiency losses and tolerances of the grid and voltage drop at inductors have not been taken into account. These would lead to a further increase in practice.

Table 14: Calculation of the minimum DC voltage for transformerless, single-stage inverters

Switching pattern	Formula	400 $V_{AC,LL}$	600 $V_{AC,LL}$
W/o third harmonic	$U_{ZK} = U_{AC,LL,eff} \cdot \frac{\sqrt{2}}{\sqrt{3}} \cdot 2$	653 V	980 V
With third harmonic	$U_{ZK,CM} = U_{AC,LL,eff} \cdot \sqrt{2}$	565 V	848 V

Operating points of the PV generator below this voltage limit cannot be realized with these topologies and would therefore lead to yield losses.

In two-stage topologies with DC-DC converters as used in multi-MPPT inverters, the PV voltage is decoupled from the DC link of the inverter, which means that the operating range of the inverter is generally increased to a lower voltage. Multi-MPPT inverters can therefore theoretically lead to an increase in yield.
However, for the cases simulated in PVSyst© in the previous sections, these operating points can be neglected. If the string length was correctly designed for the climatic conditions, none of the simulation variants resulted in yield losses due to the voltage threshold of the inverter. Both scenarios were based on the parameters of a single-stage, transformerless inverter with the corresponding voltage threshold in each case. The use of a multi-MPPT inverter with a larger input voltage window would therefore not have resulted in any additional yield.
However, aging effects were not simulated in the simulations performed. In practice, these lead to reduced system voltages over the lifetime of the system. However, for the module technology considered, it could be shown in the simulation that with an annual aging of 0.55 %, the yield losses induced by the voltage limit after 25 years (in the 25th year) are only 0.1 %.
Therefore, from the authors' point of view, increasing the input voltage range does not bring any noticeable yield gain if the system is designed correctly.

Efficiency of the inverter

The efficiency of the inverter has a great influence on the total yield of a PV system, since all losses occurring in the inverter lead directly to a reduction in the yield. PVSyst© models these losses through so-called ond file. These files generally contain three efficiency curves for three different input voltages, each with 8 base points at different power levels. PVSyst© interpolates between the points (quadratically between the voltages and linearly between the power levels). The efficiencies refer to the nominal AC voltage of the inverter. The ambient temperature at which the measurement curves are measured is not clearly specified.
In general, from the authors' point of view, it should be noted that when comparing a single-stage system with a two-stage system (cf. Figure 1), a reduced efficiency can be expected overall. It can also generally be assumed that the component effort of the overall system and thus the costs will increase. The data stored in PVSyst© does not reflect this point. From the authors' point of view, however, this is mainly due to the accuracy and origin of the efficiency data (see next point).

Reliability of efficiency data

The data is generally provided by the manufacturer of the inverter. PVSyst© does not check these values and accepts no liability here. When checking two inverters from different manufacturers, it was found that in both cases there were average deviations of 0.3 to 0.4 % points between measurements and the values specified in the ond. file. The measurements for this comparison were carried out at Fraunhofer ISE in the TestLab Power Electronics[1]. Since the efficiencies of current inverters are very high overall, a comparison of different inverters in PVSyst© is heavily dependent on the reliability of the inverter data. Due to the origin of the data, a comparison of efficiency curves with similar values close to each other is therefore not reliable according to the authors opinion.
In practice, decisions on which inverter to use are influenced not only by costs but also by the results of yield simulations. The interest of the manufacturers to be as good as possible here is correspondingly high. Whether these results also correspond to the practice is impossible to evaluate after the construction of the plant, since the plant is built only with one of the selected inverters. Due to the aforementioned inaccuracy of the data and the very similar efficiency curves, it is therefore questionable from the

[1] https://www.ise.fraunhofer.de/de/fue-infrastruktur/akkreditierte-labs/testlab-power-electronics.html

authors' point of view whether a comparison of inverters in PVSyst© leads to realistic results.
When doing a yield analysis in PVSyst© or other software with different inverters this fact should always be taken into account.
Additional, since the curves are only available for the nominal AC voltage, a simulative comparison of inverters at voltages other than the nominal AC voltage is also not meaningful from the authors' point of view.

Modeling of Multi-MPPT inverters in PVSyst©

The efficiencies of multi-MPPT inverters are given in the data sheet and in the ond file for a symmetrical loading of the DC inputs for the entire inverter. PVSyst© scales these curves to each MPPT and then simulates each MPPT as a separate inverter. This procedure is correct for symmetrical loading of the DC inputs.
In practical designs, however, it is often the case that an asymmetrical distribution of the strings occurs. The DC inputs of the inverters are correspondingly overdimensioned. In this case, PVSyst© allows an asymmetrical scaling of the MPPTs corresponding to the DC power. This procedure is correct provided that all losses occur in the inverter stage. However, since the losses are distributed over both the DC-DC stage and inverter stage, an error occurs in the model. In the following, this error is considered using an example of an inverter with multi-MPPT. The starting point are the three efficiency curves at 860 V, 1160 V and 1300V MPP voltage or a specific multi-MPPT inverter (see appendix). The maximum efficiency occurs at the operating point when the DC-DC converter are not working and the DC link voltage is close to the minimum. In the example this is 1160 V. For this operating curve, the losses in the DC-DC converter can therefore considered as almost zero. An increase of the input voltage leads to an increase of the losses in the inverter, the losses in the DC-DC converter can be further considered as zero. At lower DC voltages, the DC-DC converter continue to maintain the DC link voltage at 1160 V. Therefore, the losses in the DC-AC stage are constant. The increase in losses in the total losses can therefore be attributed to the DC-DC converter. Therefore, from these assumptions, the curves for DC-DC converter and DC-AC stage can be modeled for 860 V DC voltage (see appendix). For further calculation, the efficiency curve was interpolated with respect to oversizing and then a parameter fit was performed based on a second degree polynomial[1] and then the error was calculated. For the selected example of a 125 kVA multi MPPT inverter with 6 MPPTs, the wiring (2 | 2 | 2 | 2 | 1 | 1) results in a relative error in the MPP of 0.04 % points.
The authors therefore consider the modeling to be sufficiently accurate. Especially against the background that no detailed efficiency data is available and the accuracies of the measured data is low.

Influence of the AC output voltage of the inverter

With multi-MPPT inverters, higher AC voltages can generally be realized due to the decoupling from the DC link and the PV voltage. Instead of 600 $V_{AC,LL}$ up to 800 $V_{AC,LL}$ are possible for a maximum module string voltage of 1500 V. For smaller roof top systems with direct connection to the public grid (400 $V_{AC,LL}$), this point has no relevance. However, for large systems with a separate AC distribution network, a higher AC voltage can lead to lower system costs. On the one hand, the cable effort required on the AC side to the sub-station is reduced. On the other hand, switchgear and transformers can be better utilized at higher AC voltages. This may lead to a reduction in costs. Due to the limited scope of the study, it was not possible to quantify this point more precisely.

[1] Schmidt, H., et al. "Modellierung der Spannungsabhängigkeit des Wechselrichter-Wirkungsgrades, 23." *Symposium Photovoltaische Energieversorgung, Bad Staffelstein, March*. 2008.

6 Conclusion

The investigations carried out in this study have shown that an estimate of the additional yield of multi-MPPT compared to single-MPPT for the simulated scenarios is possible in principle with PVSyst© for some effects. The accuracy of the solar cell models used and the modeling of the inverter efficiency is sufficiently accurate in the view of the authors if the model parameters, which are provided by the manufacturers, are correct.
The yield simulations with different timesteps (15 min and 60 in) where compared with each other and a clear difference in the histograms of the MPP voltage and power could be observed. However, the overall effects for a yield simulation for typical string layouts are rather small. In the scenario with a string length of 20 modules, a difference in the range of 0.25% of the overall yield could be observed. This effect is mainly caused by the smoothing of power spikes that have less impact when doing hourly simulations. Losses resulting from falling below the minimum MPP voltage can be neglected for all cases.
The authors are critical concerning the quality and accuracy of the databases for components contained in PVSyst©, especially the efficiency of inverters. There is no sufficient quality assurance here, so that a comparison of components with very similar curves seem to be not very reliable. In the case of the inverter in particular, large deviations from measured values for the efficiency and the model parameters were found here on a random basis.
However, since the efficiency of the inverter was not taken into account for the comparisons of the yield simulations with and without multi-MPPT, the various effects could be investigated independently of the inverter behavior. In two of the simulated scenarios, a significant increase in yield could be achieved by using multi-MPPT inverters. These include an asymmetric string configuration of the PV generator (cf. chapter 5.2) and a heterogeneous shading scenario (e.g. caused by a tree, (cf. chapter 5.7). In both cases, the yield gain was up to 1 % of the total yield. This value can be considered as a maximum yield gain. When taking the efficiency of real inverters into account, this value will probably be reduced as the efficiency of multi MPPT inverters can be assumed to be lower than the efficiencies of single-stage inverters (cf chapter 5.11).
In all other cases investigated, the possible additional yield is considerably lower and the calculated gain here is below 0.1 %. The accuracy of the efficiency curves of the inverters is significantly lower, so that the potential additional yield in these cases seems questionable. The influence of the geographical location of the PV system is relatively small and does not lead to a qualitative change of the results.
The low impact in general can be explained by the module curves at different irradiances shown in Figure 4. The MPP voltage changes only very slightly, which means that there is only a small mismatch in the case of irradiance-induced mismatch effects. The individual effects are shown again in the following figure.

Losses / Effect	Max yield gain with Multi-MPPT	Comment
heterogenous string configuration	**up to 1 %**	**Yield gain may be reduced by lower effiency of Multi-MPPT inverter**
Near Shading losses by a tree	**~ 1 %**	**Yield gain may be reduced by lower effiency of Multi-MPPT inverter**
Near Shading losses by PV table with fixed tilt	< 0.1 %	for plant with optimized PR
Near Shading losses by PV table with single axis tracking	< 0.1 %	for plant with optimized PR
Moving Clouds	*not relevant*	*Effect can be neglected*
Soiling losses	*not relevant*	*Effect can be neglected*
Module degradation (Aging)	*not relevant*	*Effect can be neglected*
Mismatch losses due to dispersion of parameters	< 0.01 %	
Mismatch due to variation of tilt	< 0.01 %	
Mismatch due to variation of orientation	< 0.1 %	
Mismatch due to inhomogenous temperature dispersion	< 0.1 %	
Ohmic DC losses (String cable length)	< 0.01 %	
Inverter losses due to efficiency	*not considered in detail*	Data quality and reliability questionable
Inverter losses due to voltage threshold	*not relevant*	No losses if string length is designed carefully
Inverter AC output voltage	*not considered in detail*	*Detailed analysis necessary*

Figure 22: Summary and evaluation of the results

In summary, it can be said that multi-MPPT can be beneficial from a yield perspective if the system configuration is very heterogeneous in terms of shading or string configurations. However, this requires a very high efficiency in the DC-DC stages of the inverter, so that the additional yield (~1 % in the cases outlined) is not reduced too much by the potentially worse efficiency of a two-stage system.
For homogeneous systems, significant additional yield from multi-MPPT is not expected. With a correct design of the string length, an increase in yield is also not to be expected due to the wider input voltage range for multi-MPPT inverters.
The calculations carried out refer entirely to calculations based on crystalline Si modules. Even when considering aging effects, this effect does not lead to yield losses over the modules lifetime due to mismatch or falling below the minimum inverter input voltage. For other PV technologies such as thin film the impact may be more relevant.
One question that is not answered in this study is whether cost savings can be achieved on system level due to the higher AC voltages of multi-MPPT inverters. This would require separate cost studies, which is beyond the scope of the study.

7
Appendix

Appendix 3.1: I-V curve modeling of PV strings

The model used in this analysis for generating the individual IV curves of the PV string is based on the model proposed by Villalva et al.[1].

Figure 23 depicts a single-diode model and the equivalent circuit of a practical PV device.

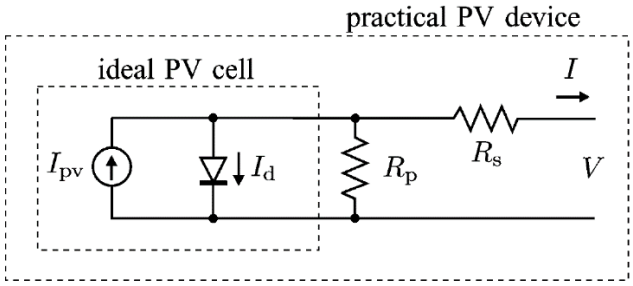

Figure 23: Single-diode model of the theoretical PV cell and equivalent circuit of a practical PV device including the series and parallel resistances. [1]

The basic equation that mathematically describes the IV characteristic of the ideal PV cell is

$$I = I_{\mathrm{PV,cell}} - I_{0,\mathrm{cell}} \left[\exp\left(\frac{q \cdot V}{a \cdot kT} \right) - 1 \right]$$

Where $I_{\mathrm{PV,cell}}$ is the current generated by the incident light (proportional to the sun irradiation), $I_{0,\mathrm{cell}}$ the reverse saturation or leakage current of the diode, q the electron charge, k the Boltzmann constant, T the temperature in kelvin and a the ideality factor for the diode. For a realistic PV array, additional losses have to be considered, which leads to the following equation:

$$I = I_{\mathrm{PV}} - I_0 \left[\exp\left(\frac{V + R_\mathrm{s} \cdot I}{V_\mathrm{t} \cdot a} \right) - 1 \right] - \frac{V + R_\mathrm{s} \cdot I}{R_\mathrm{p}}$$

Where I_{PV} is the current of the PV array/string, I_0 the reverse saturation current, R_s the series resistance, R_p the parallel resistance and V_t the thermal voltage defined as

$$V_\mathrm{t} = N_\mathrm{s} \frac{\mathrm{k} \cdot T_\mathrm{k}}{\mathrm{q}}$$

Where N_s is the number of solar cells in the PV string (in this case $N_\mathrm{s} = 72 \cdot 28$), q is the electron charge and T_k is the cell/module temperature in Kelvin.

[1] [1] M. G. Villalva, J. R. Gazoli and E. R. Filho, "Comprehensive Approach to Modeling and Simulation of Photovoltaic Arrays," in IEEE Transactions on Power Electronics, vol. 24, no. 5, pp. 1198-1208, May 2009, doi: 10.1109/TPEL.2009.2013862.

The equation for the IV curve is an implicit function which cannot be solved analytically. However, it can be made numerically explicit so that

$$I = f(V)$$

PVsyst uses additionally a scaling factor mua for the diode ideality factor

$$a = a_0 + mua \cdot \Delta T$$

Where ΔT is the deviation to the STC temperature. Furthermore, PVsyst uses a thermal current coefficient (named $muISC$ in the PVsyst model), which scales the PV cell current

$$I_{\mathrm{PV,cell}} = \left(I_{\mathrm{PV,n}} + muISC \cdot \Delta T\right) \cdot \frac{G}{G_{\mathrm{n}}}$$

Where $I_{\mathrm{PV,n}}$ is the cell current at STC temperature, G_{n} the nominal value of irradiation (1000 W/m²) and G the currently observed irradiation on the cell surface.

In the same manner, a thermal voltage coefficient (named $muVoc$ in the PVsyst model) is used in order to account for the thermal dependance of the open circuit voltage.

PVsyst also includes a dependence of the parallel resistance R_{p} on the irradiation G:

$$R_{\mathrm{p,eff}} = R_{\mathrm{p}} + \left(R_{\mathrm{p0}} - R_{\mathrm{p}}\right) \cdot \exp\left(-R_{\mathrm{p,exp}} \cdot \frac{G}{G_{\mathrm{n}}}\right)$$

With R_{p} as the parallel resistance of the standard model, R_{p0} the parallel resistance at zero irradiation and $R_{\mathrm{p,exp}}$ the exponential factor (5.5 for c-Si modules).

With this model, the IV curve for strings of solar cells / modules can be generated depending on the environmental conditions. All parameters can be directly extracted from the PVsyst model of the manufacturer of the solar module.

PVsyst models the degradation of the solar modules in such a manner, that the overall degradation affects both the voltage and the current of the IV curve. Consultation with PVsyst SA revealed, that the degradation is accounted by 50% to the voltage and by 50% to the current. This can be included in the model as following:

$$f_{\mathrm{deg}} = \sqrt{1 - deg}$$

Where f_{deg} is the factor used to scale both the voltage and current of the IV curve and deg is the degradation of the module.

Appendix 3.3: Modelled I-V-curves for Canadian Solar CS3W-410P 1500V

I-P-curves for different irradiances

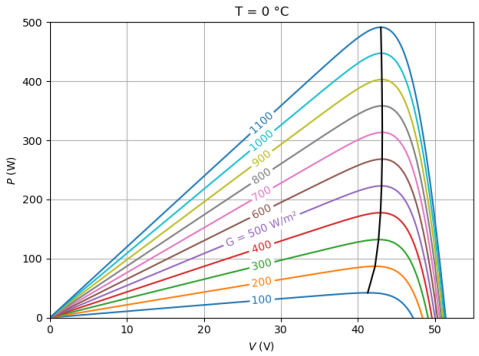

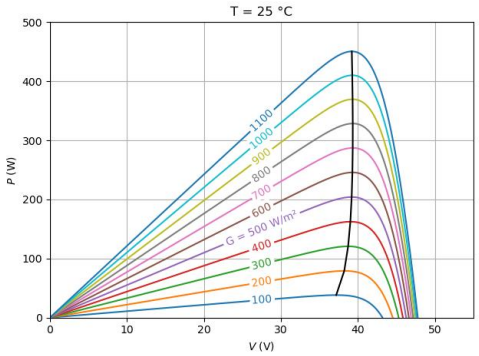

Figure 24: Modeled P-V-curves for different irradiances with single diode model for Canadian Solar CS3W-410P 1500V (cell temperature: 0 °C, left – 25 °C right)

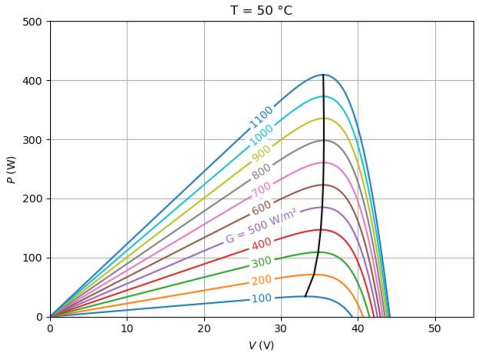

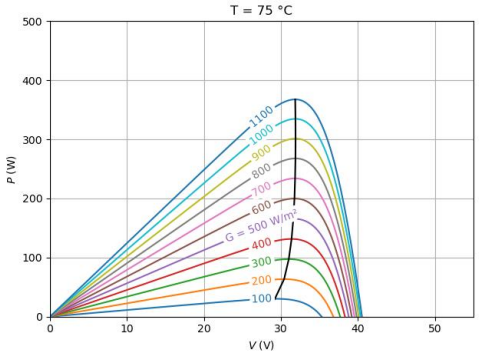

Figure 25: Modeled P-V-curves for different irradiances with single diode model for Canadian Solar CS3W-410P 1500V (cell temperature: 50 °C, left; – 75 °C right)

P-I-curves for different temperatures

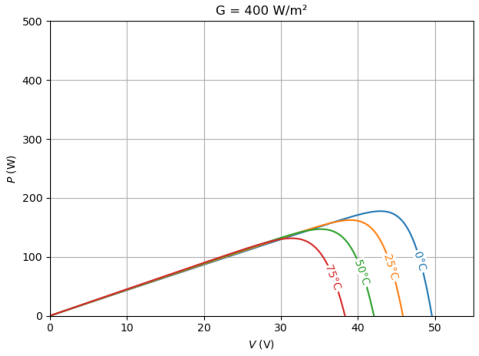

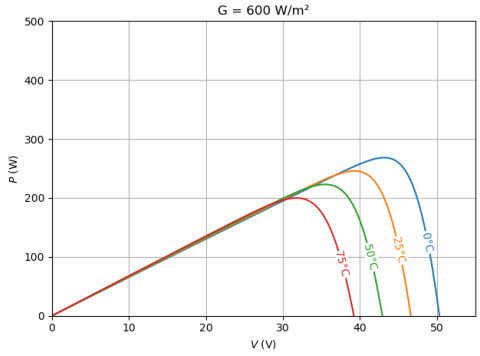

Figure 26: Modeled P-V-curves for different cell temperatures with single diode model for Canadian Solar CS3W-410P 1500V (400 W/m², left; – 600 W/m² right)

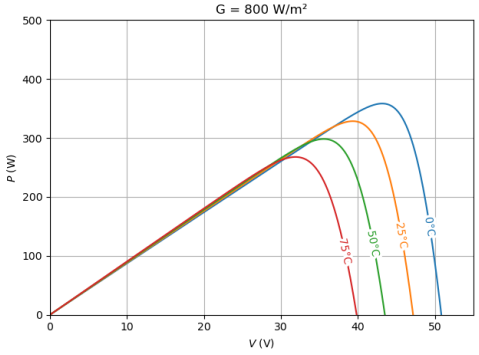

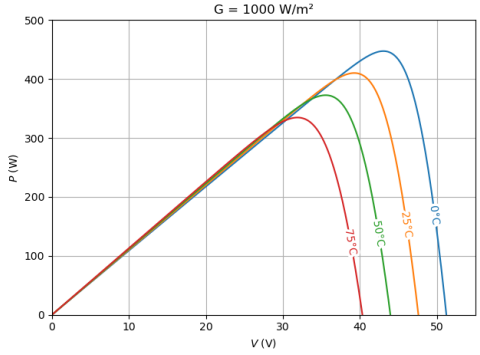

Figure 27: Modeled P-V-curves for different cell temperatures with single diode model for Canadian Solar CS3W-410P 1500V (800 W/m², left; – 1000 W/m² right)

P-V-curves for different temperatures with temperature model

The plots are for different ambient temperatures. The actual cell temperature are calculated according to the following formula:

$$T_{\mathrm{cell}} = T_{\mathrm{amb}} + \frac{\alpha\, G_{\mathrm{inc}}(1-\eta)}{U}$$

Where T_{cell} is the cell temperature used to model the IV curve, T_{amb} is the ambient temperature, α is the absorption coefficient of solar radiation of the PV module (usually assumed with 0.9 in PVSyst©), G_{inc} the irradiance on the PV module, η the efficiency of the PV module (the STC module efficiency from datasheet was used in this case) and U the thermal loss factor (assumed to be constant with the value of $U = 29\,\mathrm{W/(m^2K)}$). This value for *U* equals an additional temperature at the cells compared to the ambient temperature of 25.2 K at 1000 W/m² of irradiation.

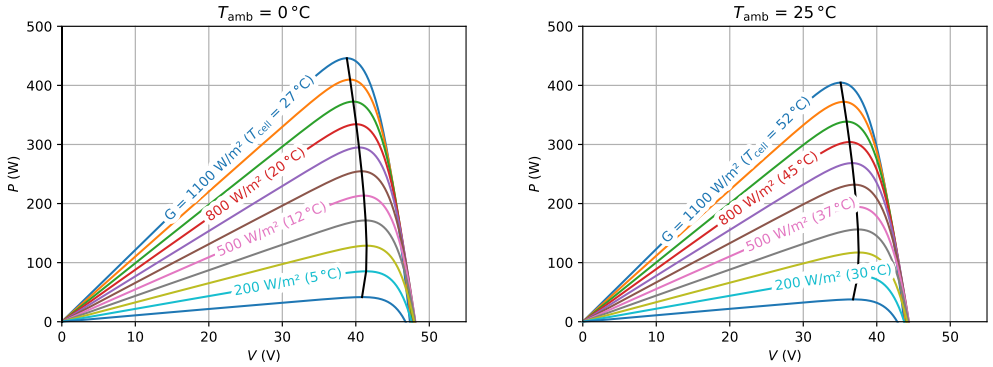

Figure 28: Modeled P-V-curves for different irradiances and self-heating taken into account with single diode model for Canadian Solar CS3W-410P 1500V (ambient temperature: 0 °C, left; 25 °C right)

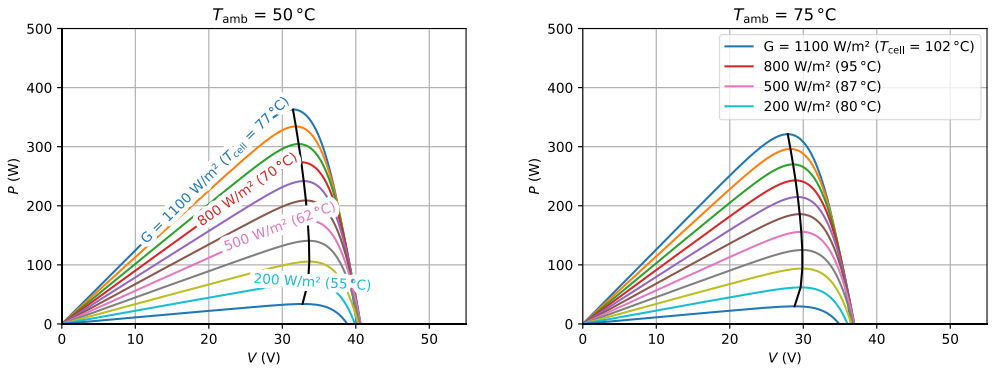

Figure 29: Modeled P-V-curves for different irradiances and self-heating taken into account with single diode model for Canadian Solar CS3W-410P 1500V (ambient temperature: 50 °C, left; 75 °C right)

Appendix 4.3: Results for yield simulation with different time steps for string length of 18 modules

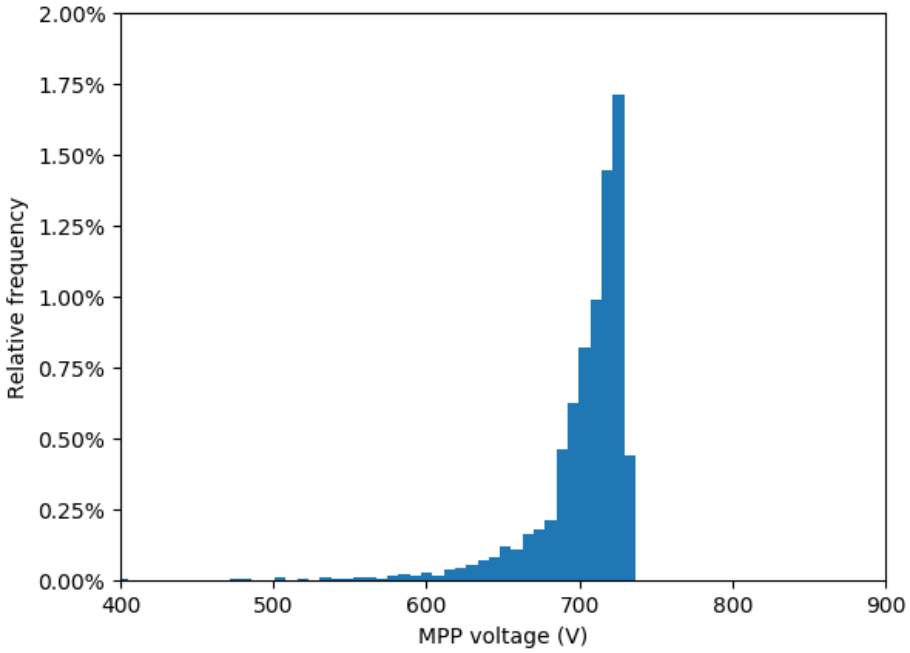

Figure 30: Histogram for the distribution of the MPP voltages in the year 2016 for a string with 18 modules and 60 min timesteps.

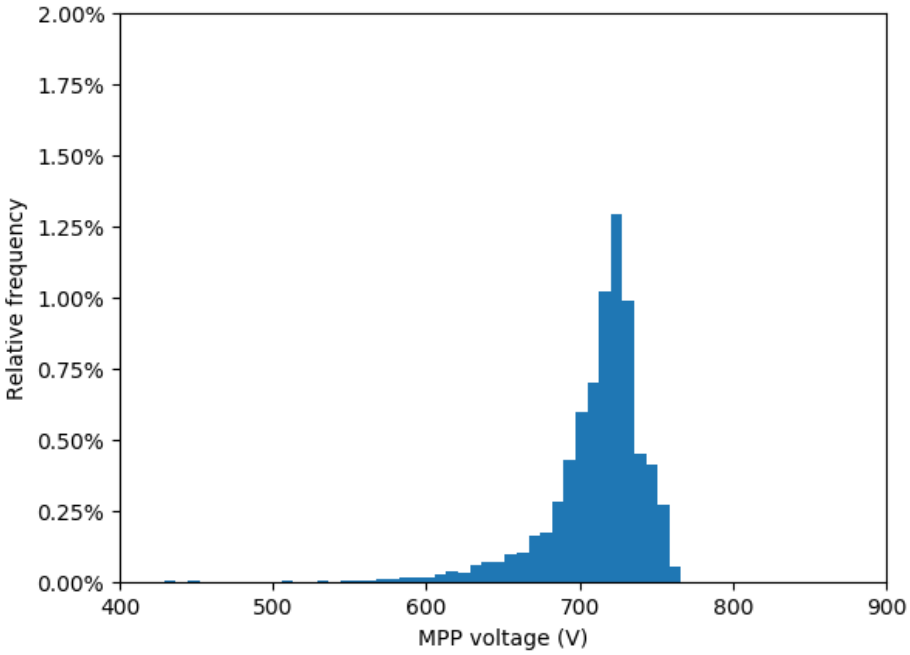

Figure 31: Histogram for the distribution of the MPP voltages in the year 2016 for a string with 18 modules and 15 min timesteps.

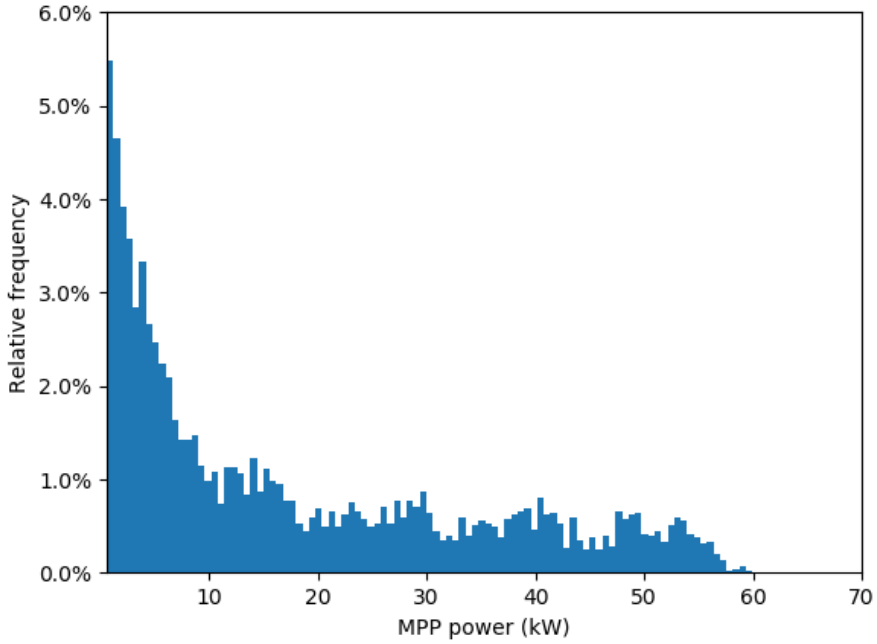

Figure 32: Histogram for the distribution of the MPP power in the year 2016 for a string with 18 modules and 60 min timesteps.

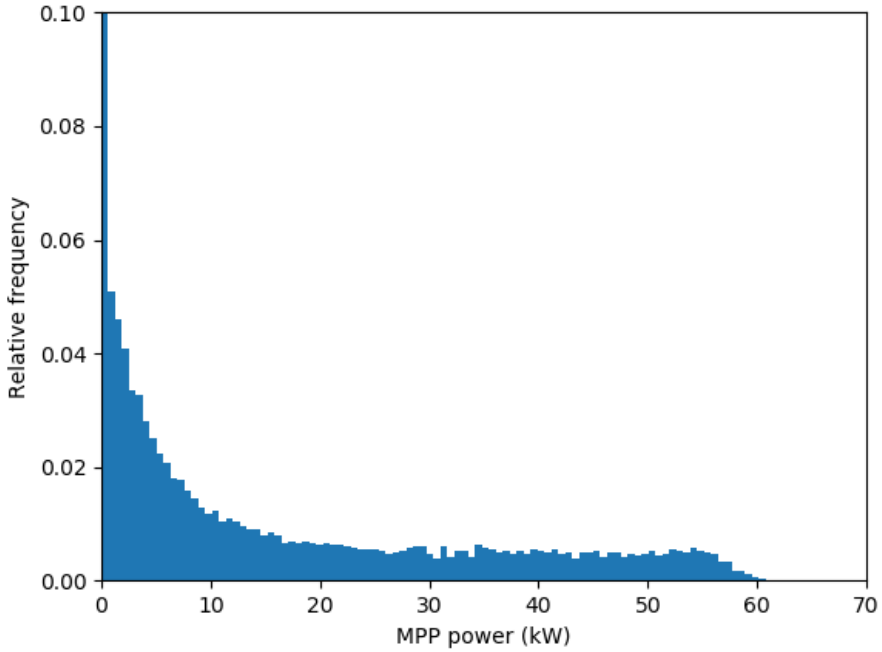

Figure 33: Histogram for the distribution of the MPP power in the year 2016 for a string with 18 modules and 15 min timesteps.

Appendix 5.1: Optimum tilt at Arkona and Abu Dhabi

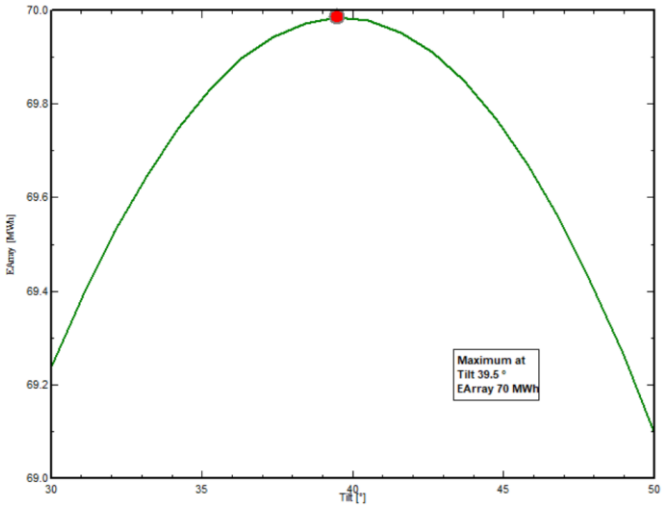

Figure 34: Tilt optimization for Arkona

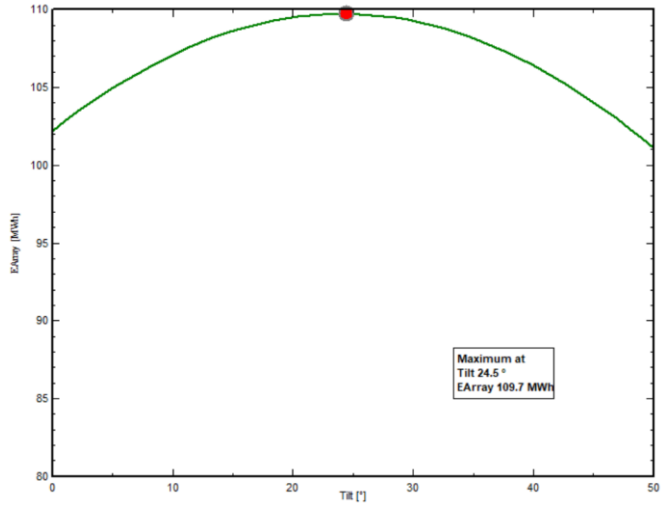

Figure 35: Tilt optimization for Abu Dhabi

Appendix 5.2: Synthetically generated curves for different configurations of the solar generator

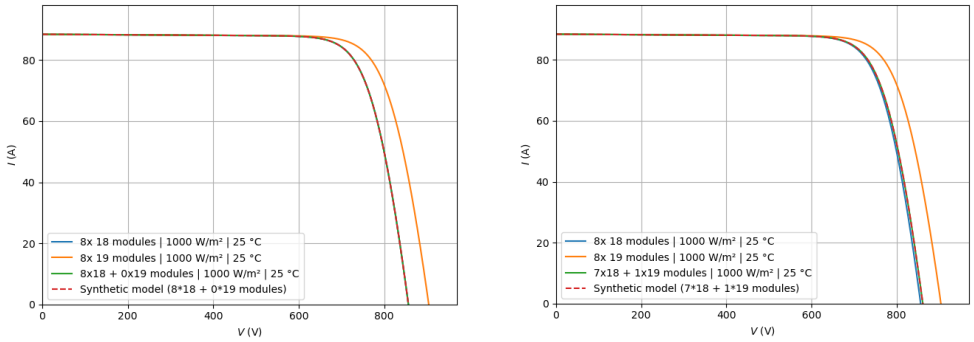

Figure 36: Synthetically generated curves for different configurations of the solar generator (8x 18 + 0x 19, left – 7x 18 + 1x 19, right)

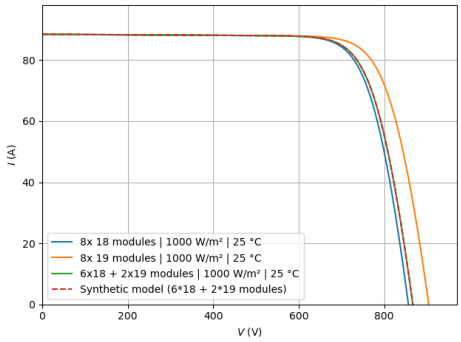

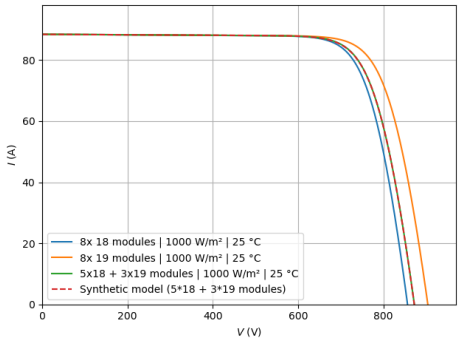

Figure 37: Synthetically generated curves for different configurations of the solar generator (6x 18 + 2x 19, left; 5x 18 + 3x 19, right)

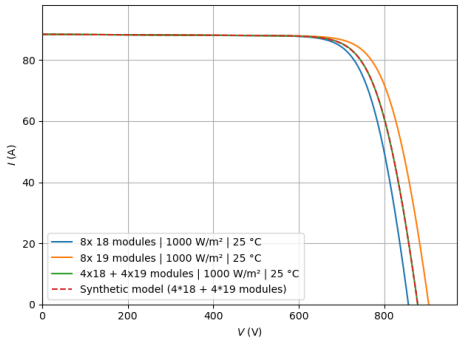

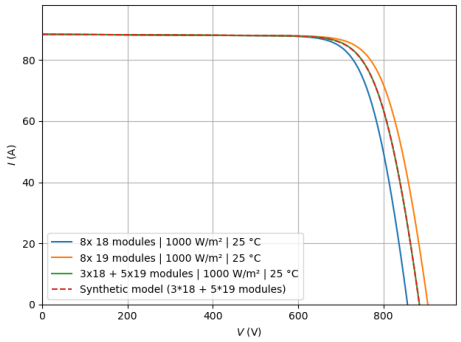

Figure 38: Synthetically generated curves for different configurations of the solar generator (4x 18 + 4x 19, left; 3x 18 + 5x 19, right)

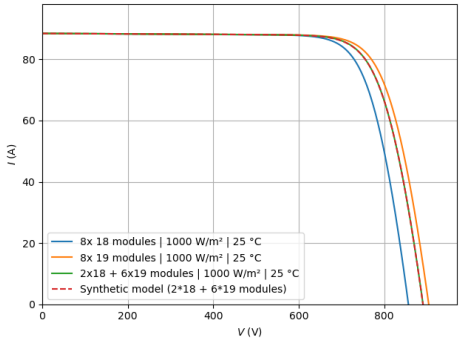

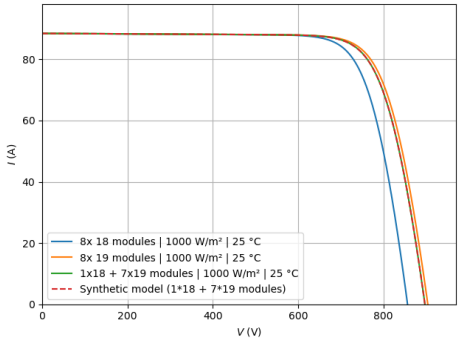

Figure 39: Synthetically generated curves for different configurations of the solar generator (2x 18 + 6x 19, left; 1x 18 + 7x 19, right)

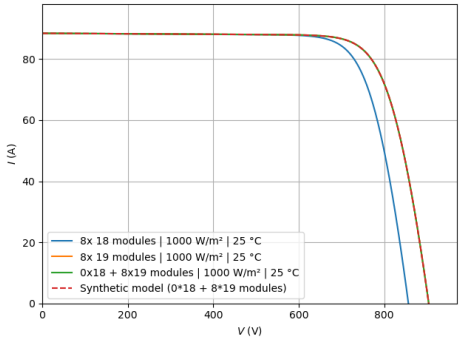

Figure 40: Synthetically generated curves for different configurations of the solar generator (0x 18 + 8x 19)

Appendix 5.2: Overview of PVsyst models used in this chapter

Project name in PVsyst: KacoStudy_RT_60kVA_Arkona_UnsymPVGenerator

Var.	Scenario	MPPT	String configuration
VC0	A	Single	9: 0x 18 + 8x 19
VC1	A	Single	1: 8x 18 + 0x 19
VC2	A	Multi #6	2: 7x 18 + 1x 19
VC3	A	Multi #6	3: 6x 18 + 2x 19
VC4	A	Multi #6	4: 5x 18 + 3x 19
VC5	A	Multi #6	5: 4x 18 + 4x 19
VC6	A	Multi #6	6: 3x 18 + 5x 19
VC7	A	Multi #6	7: 2x 18 + 6x 19
VC8	A	Multi #6	8: 1x 18 + 7x 19
VC9	A	Single	2: 7x 18 + 1x 19
VCA	A	Single	3: 6x 18 + 2x 19
VCB	A	Single	4: 5x 18 + 3x 19
VDC	A	Single	5: 4x 18 + 4x 19
VDD	A	Single	6: 3x 18 + 5x 19
VDE	A	Single	7: 2x 18 + 6x 19
VDF	A	Single	8: 1x 18 + 7x 19
VDH	A	Multi #4	2: 7x 18 + 1x 19

Appendix 5.3: PV generator characteristic curve for scenario A with statistical normal distribution of I_{SC} and 3%

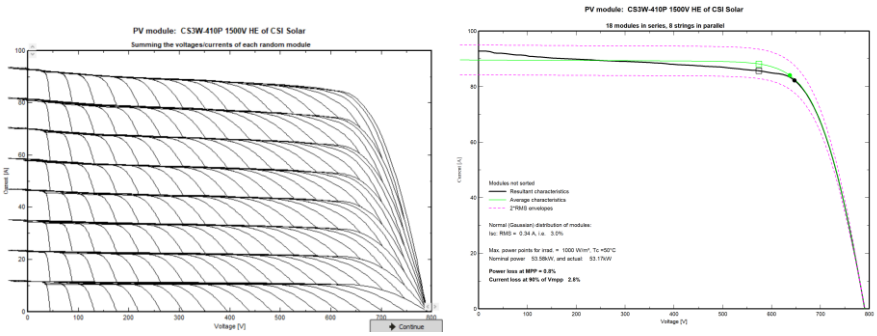

Figure 41: PV generator characteristic curve for scenario A with statistical normal distribution of Voc and 3 % deviation (left) - Resulting characteristic curve of the generator and comparison to the characteristic curve without tolerance (right)

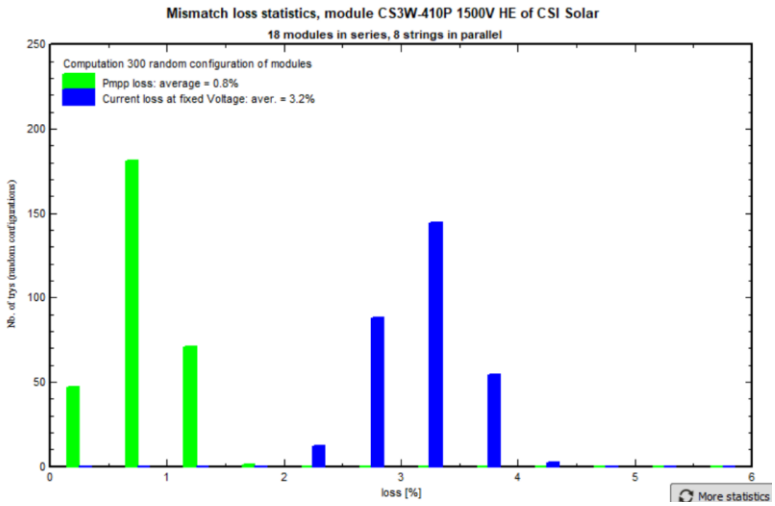

Figure 42: Histogram for 440 random arrangement in scenario A with a tolerance of 3 % in voltage

Appendix 5.4: Mismatch losses with different string lengths

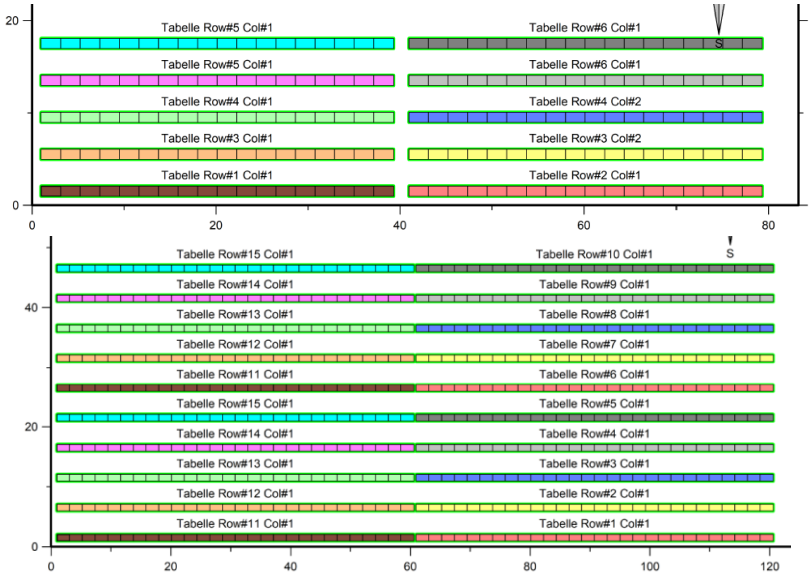

Figure 43: Size of generalized plant for scenario A (P_{DC}/P_{AC} = 1.2)

Figure 44: Size of generalized plant for scenario B (P_{DC}/P_{AC} = 1.4)

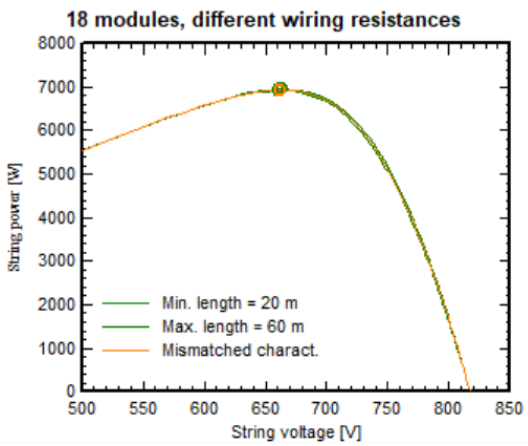

Results

	Voltage	Current	Power
String # 1	663.8 V	10.48 A	**6958.7 W**
String # 2	661.0 V	10.48 A	**6925.7 W**
Mismatched string	662.4 V	10.48 A	**6940.3 W**
Average power #1 and #2			**6942.2 W**
Mismatch power loss			**1.9W , i.e. 0.03%**

Figure 45: P-V curve for 2 different string length (left) and resulting mismatch in MPP (right) for scenario A

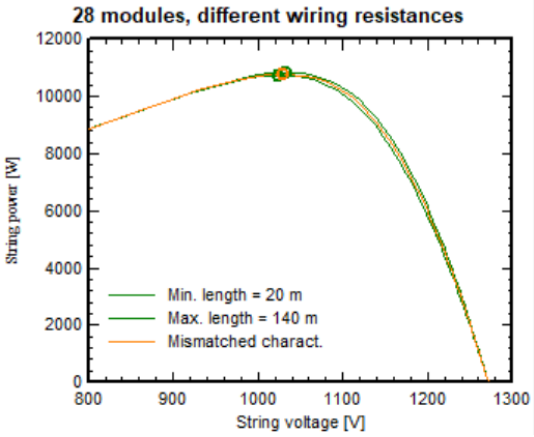

Results

	Voltage	Current	Power
String # 1	1033.4 V	10.48 A	**10833.9 W**
String # 2	1025.1 V	10.47 A	**10734.8 W**
Mismatched string	1029.2 V	10.47 A	**10779.6 W**
Average power #1 and #2			**10784.4 W**
Mismatch power loss			**4.7W , i.e. 0.04%**

Figure 46: P-V curve for 2 different string length (left) and resulting mismatch in MPP (right) for scenario B

Appendix 5.5: Mismatch losses due to inhomogeneous temperature distribution in the field

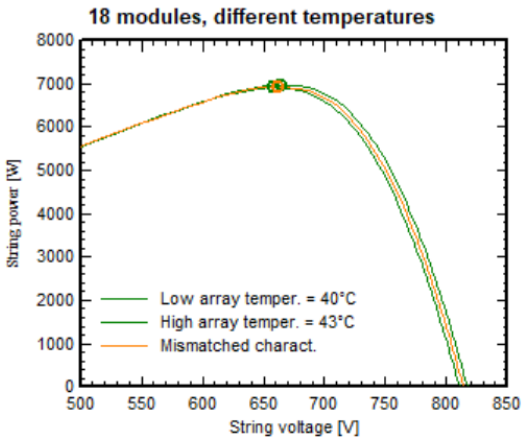

Results

	Voltage	Current	Power
String # 1	665.2 V	10.49 A	**6975.3 W**
String # 2	658.4 V	10.49 A	**6906.4 W**
Mismatched string	661.8 V	10.48 A	**6937.2 W**
Average power #1 and #2			**6940.8 W**
Mismatch power loss			**3.6W , i.e. 0.05%**

Figure 47: P-V curve for 2 different string length (left) and resulting mismatch in MPP (right) for scenario A and temperature difference 0f 2,5 K

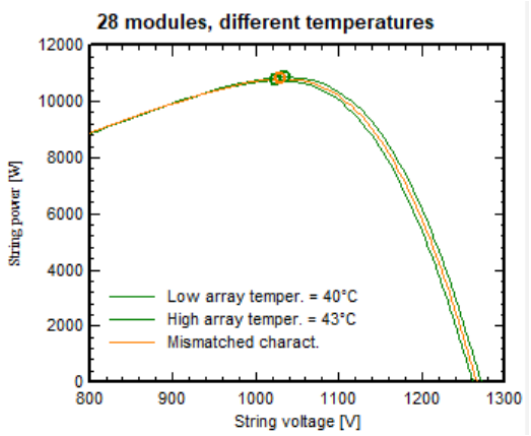

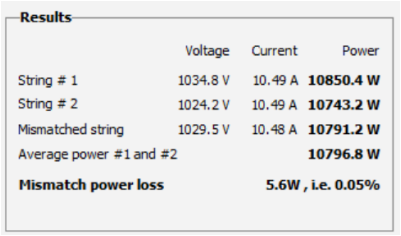

Figure 48: P-V curve for 2 different string length (left) and resulting mismatch in MPP (right) for scenario B and temperature difference of 2,5 K

Appendix 5.6: Overview of PVsyst models used in this chapter

Variation of orientation

Location: Arkona
Project name in PVsyst: KacoStudy_RT_60kVA_Arkona

Var.	MPPT	Orientation	String configuration	P_{DC}/P_{AC}	Tilt
VC7	Single	East-West	E: 4 / W: 4	1	20 °
VC8	M6	East-West	E: 4 / W: 4	1	20 °
VC9	Single	East-West	E: 5 / W: 5	1.2	20 °
VCA	M6	East-West	E: 5 / W: 5	1.2	20 °
VCJ	Single	East-West	E: 1 / W: 9	1.2	20 °
VCK	M6	East-West	E: 1 / W: 9	1.2	20 °
VCB	Single	S: +2° / -2°	+2°: 4 / -2°: 4	1	40 °
VCC	M6	S: +2° / -2°	+2°: 4 / -2°: 4	1	40 °
VCD	Single	S: +10° / -10°	+10°: 4 / -10°: 4	1	40 °
VCE	M6	S: +10° / -10°	+10°: 4 / -10°: 4	1	40 °

Location: Abu Dhabi
Project name in PVsyst: KacoStudy_RT_60kVA_AbuDhabi

Var.	MPPT	Orientation	String configuration	P_{DC}/P_{AC}	Tilt
VC4	Single	East-West	E: 5 / W: 5	1.2	20 °
VC5	M6	East-West	E: 5 / W: 5	1.2	20 °
VC6	Single	East-West	E: 4 / W: 4	1	20 °

VC7	M6	East-West	E: 4 / W: 4	1	20 °
VCC	Single	East-West	E: 1 / W: 9	1.2	20 °
VCD	M6	East-West	E: 1 / W: 9	1.2	20 °

Variation of Tilt

Location: Arkona
Project name in PVsyst: KacoStudy_RT_60kVA_Arkona

Var.	MPPT	Orientation	String configuration	P_{DC}/P_{AC}	Tilt
VCF	Single	South	35°: 4 / 45°: 4	1	35° / 45°
VCG	Single	South	35°: 4 / 45°: 4	1	35° / 45°
VCH	Single	South	15°: 4 / 35°: 4	1	20° / 40°
VCI	M6	South	15°: 4 / 35°: 4	1	20° / 40°

Location: Abu Dhabi
Project name in PVsyst: KacoStudy_RT_60kVA_AbuDhabi

Var.	MPPT	Orientation	String configuration	P_{DC}/P_{AC}	Tilt
VC8	Single	South	20°: 4 / 30°: 4	1	20° / 30°
VC9	M6	South	20°: 4 / 30°: 4	1	20° / 30°
VCA	Single	South	15°: 4 / 35°: 4	1	15° / 35°
VCB	M6	South	15°: 4 / 35°: 4	1	15° / 35°

Appendix 5.7: Near Shading losses

Near shading by a tree

Overview of PVsyst models used in this chapter

Location: Arkona (Scenario A)
Project name in PVsyst: KacoStudy_RT_60kVA_Arkona

Var.	MPPTs	Orientation	String configuration	P_{DC}/P_{AC}	Tilt
VCL	Single	South	8 x 18 Modules	1	40 °
VCM	Multi #6	South	8 x 18 Modules	1	40 °

Location: Abu Dhabi (Scenario A)
Project name in PVsyst: KacoStudy_RT_60kVA_AbuDhabi

Var.	MPPTs	Orientation	String configuration	P_{DC}/P_{AC}	Tilt
VCE	Single	South	8 x 18 Modules	1	22 °
VCF	Multi #6	South	8 x 18 Modules	1	22 °

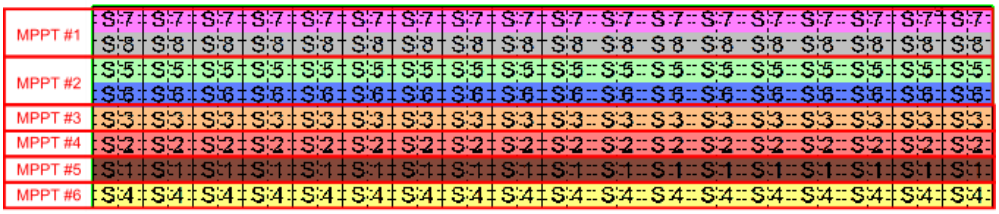

Figure 49: String configuration for Multi-MPPT for both locations

Shading scene with a tree in Arkona (scenario A)

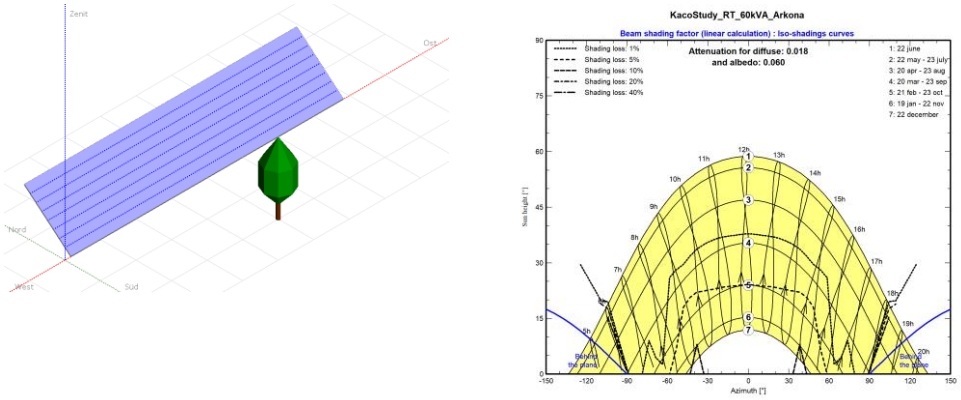

Figure 50: Shading Scene in Arkona (left) and corresponding shading diagram for single MPPT (scenario A)

Shading scene with a tree in Abu Dhabi (scenario A)

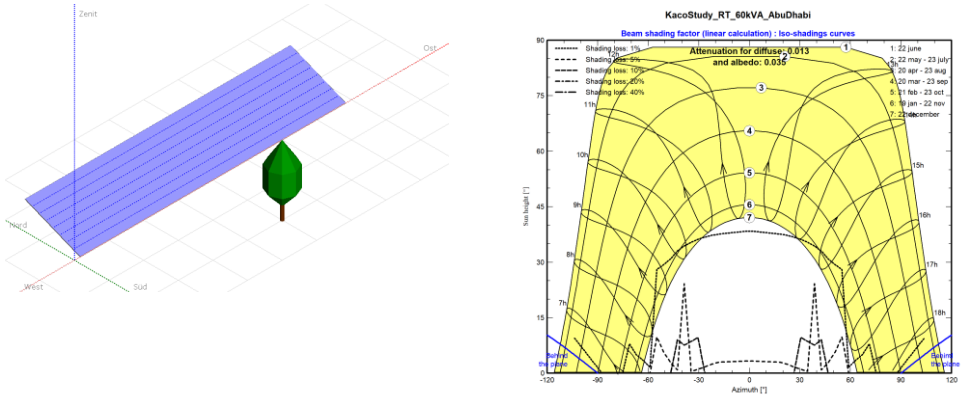

Figure 51: Shading Scene in Abu (left) and corresponding shading diagram for single MPPT (scenario A)

Near shading by module tables for PV generator with fixed tilt (Scenario B)

Overview of PVsyst models used in this chapter

Location: Arkona (Scenario B)
Project name in PVsyst: KacoStudy_GM_165kVA_Arkona

Var.	MPPTs	Orientation	String configuration	Pitch	Tilt
VC5	Single	South	15 x 29 Modules	16 m	40 °
VC6	M9	South	15 x 29 Modules	16 m	40 °
VC7	Single	South	15 x 29 Modules	8 m	40 °
VC8	M9	South	15 x 29 Modules	8 m	40 °

Location: Abu Dhabi (Scenario B)
Project name in PVsyst: KacoStudy_RT_165kVA_AbuDhabi

Var.	MPPTs	Orientation	String configuration	Pitch	Tilt
VC5	Single	South	15 x 29 Modules	6 m	22 °
VC6	M9	South	15 x 29 Modules	6 m	22 °
VC7	Single	South	15 x 29 Modules	5 m	22 °
VC8	Multi #9	South	15 x 29 Modules	5 m	22 °

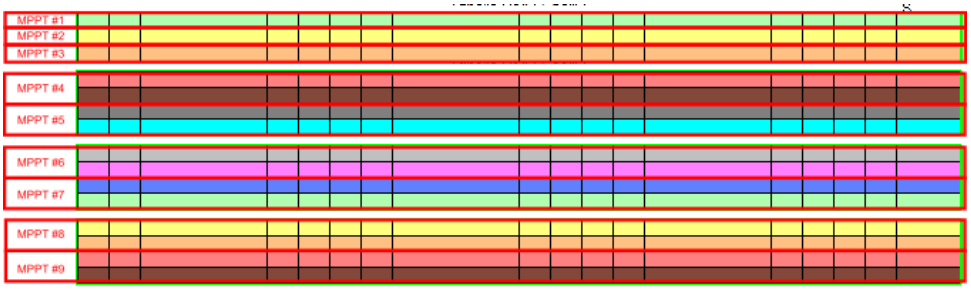

Figure 52: String configuration for Multi-MPPT for both locations

Shading scene by module tables in Arkona (scenario B)

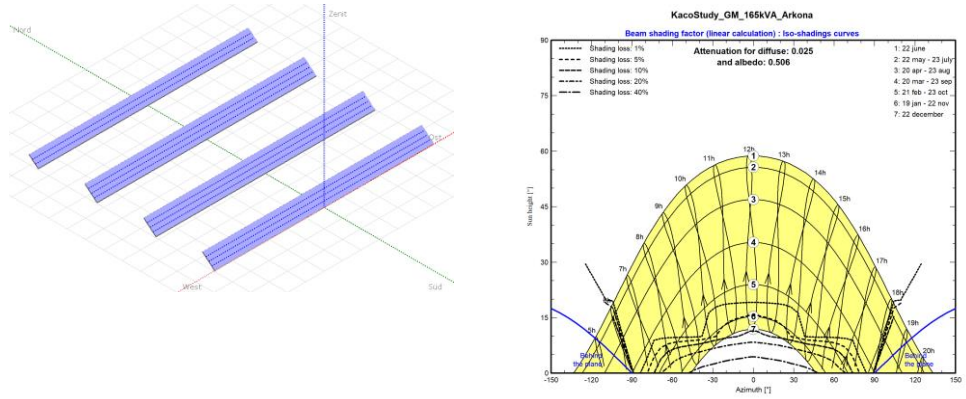

Figure 53: Shading Scene in Arkona (left) and corresponding shading diagram for 16 m pitch (scenario B)

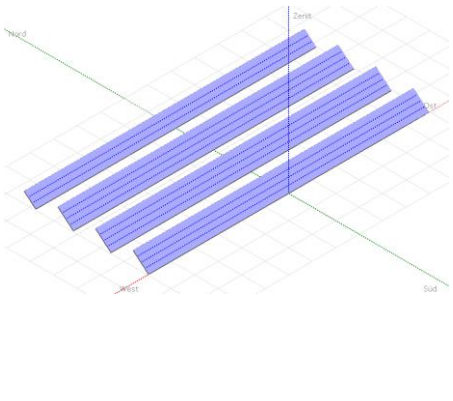

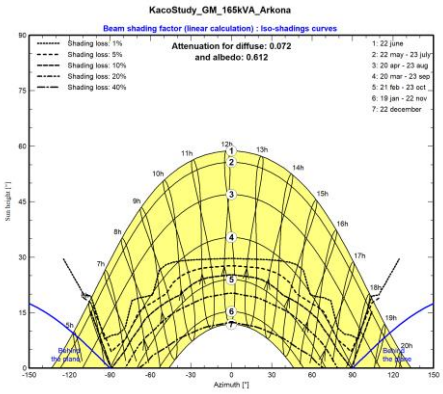

Figure 54: Shading Scene in Arkona (left) and corresponding shading diagram for 8 m pitch (scenario B)

Shading scene by module tables in Abu Dhabi (scenario B)

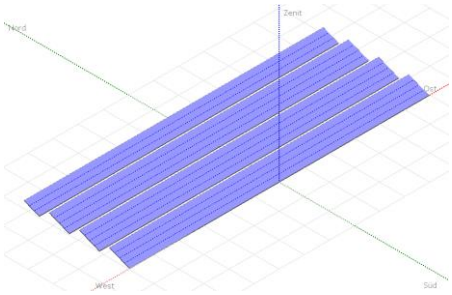

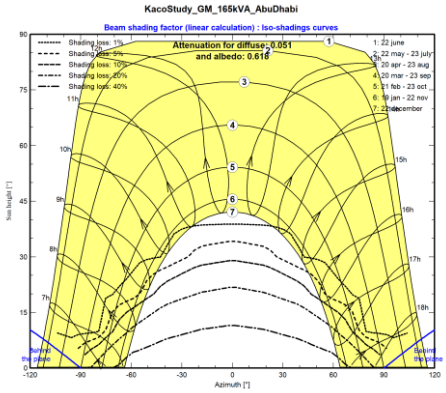

Figure 55: Shading Scene in Abu Dhabi (left) and corresponding shading diagram for 6 m pitch (scenario B)

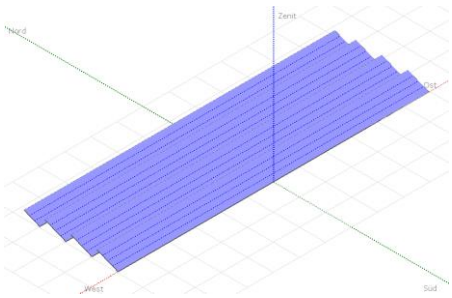

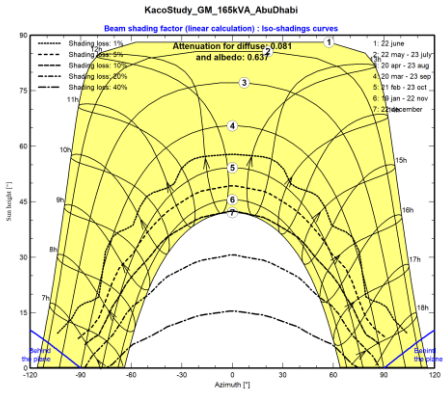

Figure 56: Shading Scene in Abu Dhabi (left) and corresponding shading diagram for 5 m pitch (scenario B)

Near shading by module tables for PV generator with single axis tracker (Scenario B)

Overview of PVsyst models used in this chapter

Location: Arkona (Scenario B)
Project name in PVsyst: KacoStudy_GM_165kVA_Arkona

Var.	MPPTs	Orientation	String configuration	Pitch	Tilt
VCF	Single	E-W-Tracker	16 x 29 Modules	10 m	-60° + 60°
VCG	M9	E-W-Tracker	16 x 29 Modules	10 m	-60° + 60°
VCJ	Single	E-W-Tracker	16 x 29 Modules	7 m	-60° + 60°
VCK	M9	E-W-Tracker	16 x 29 Modules	7 m	-60° + 60°
VCL	Single	E-W-Tracker	16 x 29 Modules	5 m	-60° + 60°
VCM	M9	E-W-Tracker	16 x 29 Modules	5 m	-60° + 60°

Location: Abu Dhabi (Scenario B)
Project name in PVsyst: KacoStudy_RT_165kVA_AbuDhabi

Var.	MPPTs	Orientation	String configuration	Pitch	Tilt
VCF	Single	E-W-Tracker	16 x 28 Modules	5 m	-60° + 60°
VCG	M9	E-W-Tracker	16 x 28 Modules	5 m	-60° + 60°
VCH	Single	E-W-Tracker	16 x 28 Modules	4 m	-60° + 60°
VCI	M9	E-W-Tracker	16 x 28 Modules	4 m	-60° + 60°
VCJ	Single	E-W-Tracker	16 x 28 Modules	3 m	-60° + 60°
VCK	M9	E-W-Tracker	16 x 28 Modules	3 m	-60° + 60°

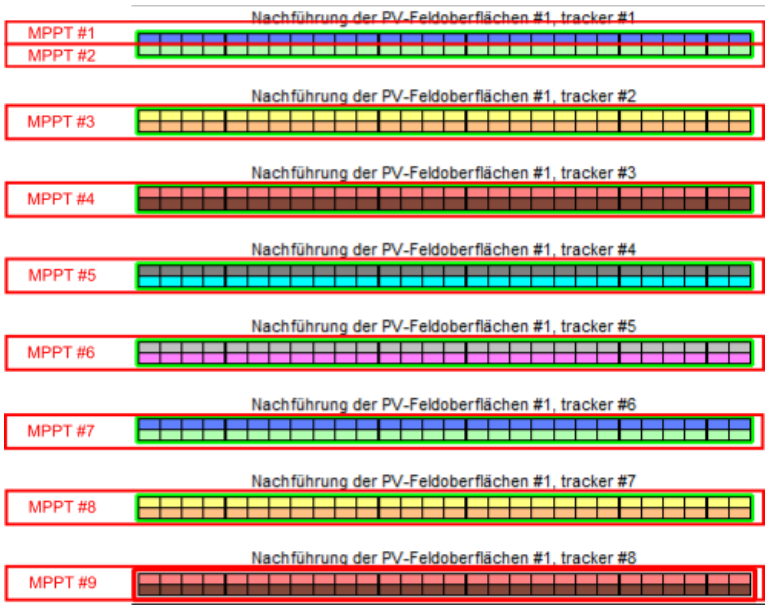

Figure 57: String configuration for Multi-MPPT for both locations

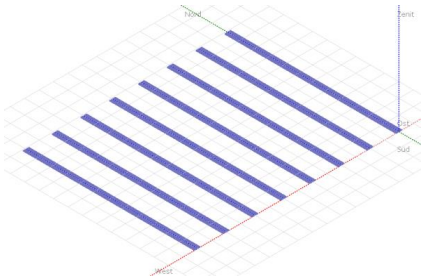

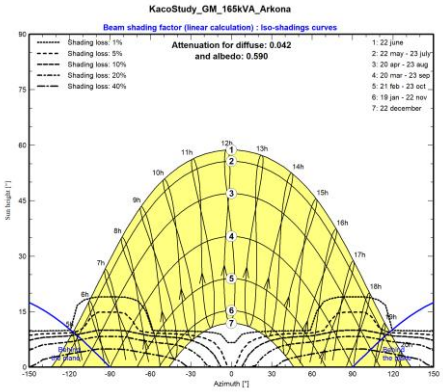

Figure 58: Shading Scene in Arkona (left) and corresponding shading diagram for 10 m pitch (scenario B)

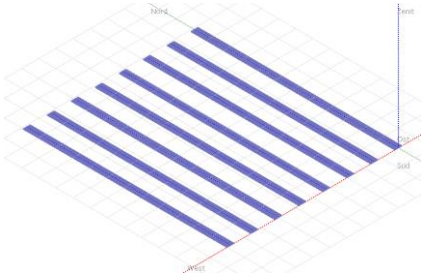

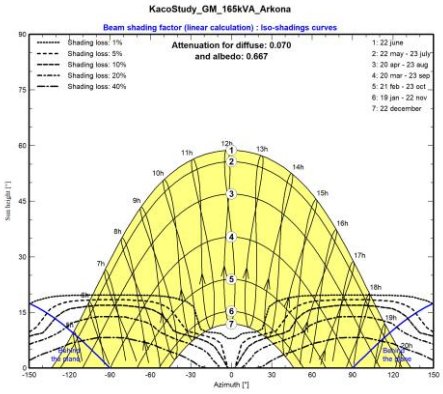

Figure 59: Shading Scene in Arkona (left) and corresponding shading diagram for 7 m pitch (scenario B)

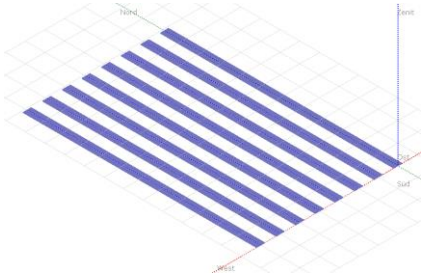

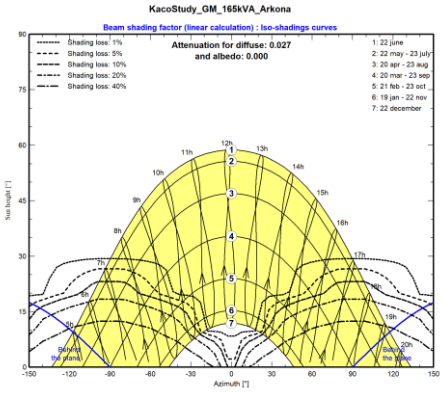

Figure 60: Shading Scene in Arkona (left) and corresponding shading diagram for 5 m pitch (scenario B)

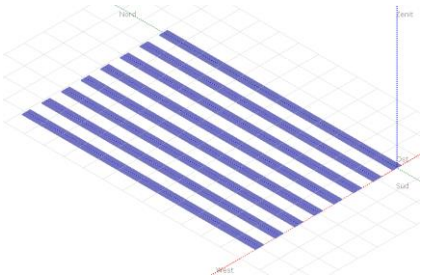

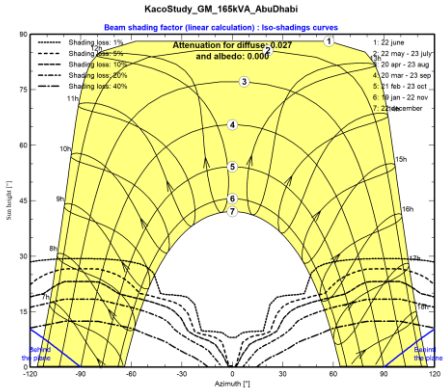

Figure 61: Shading Scene in Abu Dhabi (left) and corresponding shading diagram for 6 m pitch (scenario B)

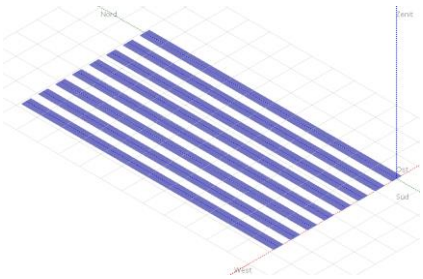

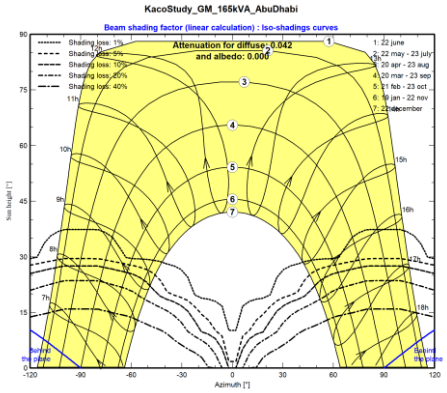

Figure 62: Shading Scene in Abu Dhabi (left) and corresponding shading diagram for 4 m pitch (scenario B)

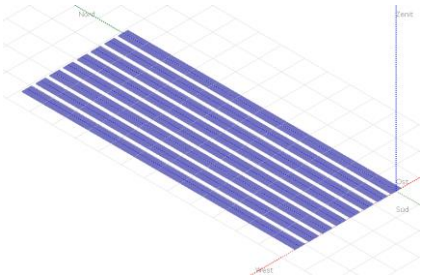

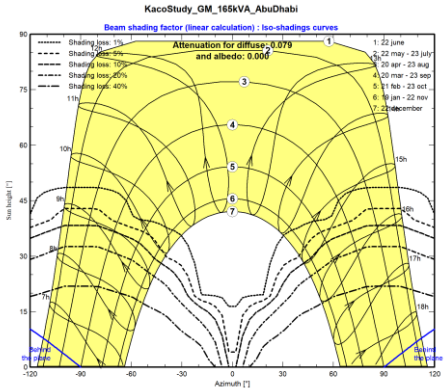

Figure 63: Shading Scene in Abu Dhabi (left) and corresponding shading diagram for 3 m pitch (scenario B)

Appendix 5.11: Efficiency modeling in PVSyst©

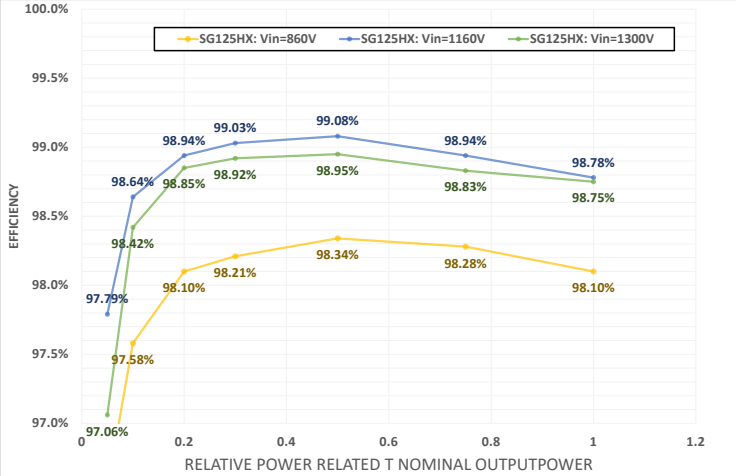

Figure 64: Efficiency curves corresponding to ond-file for different voltages for Sungrow SG125HX with 6 MPPTs

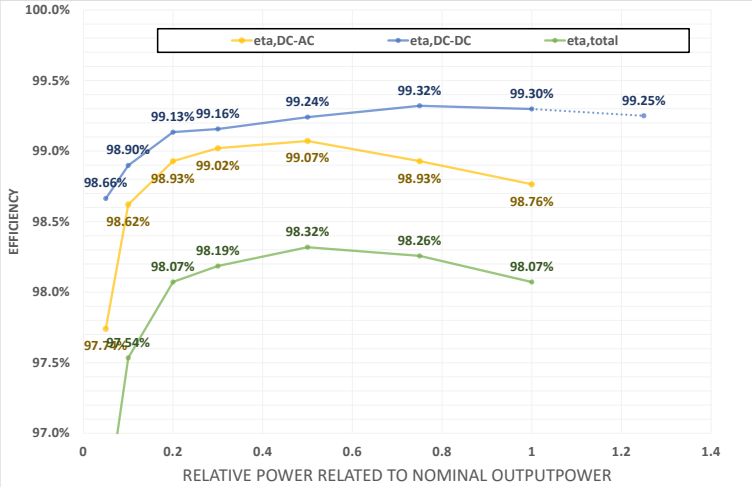

Figure 65: Efficiency of DC-DC-Stage (interpolated for p = 1.2) and DC-AC-stage for 860 V DC voltage

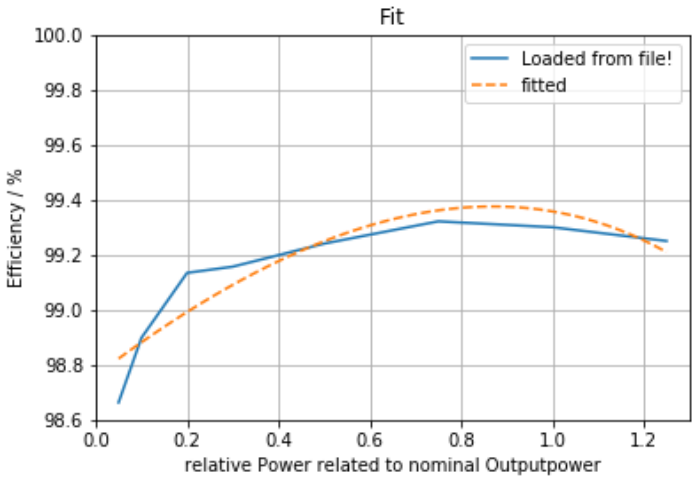

Figure 66: Curve fit for efficiency of DC-DC-stage at 860 V